Journal of Paleontology, page 1 of 25

Published by Cambridge University Press
on behalf of Paleontological Society
0022-3360/24/1937-2337
doi: 10.1017/jpa.2023.83

JOURNAL OF PALEONTOLOGY
A PUBLICATION OF THE Paleontological SOCIETY

Organic-walled microfossils from the Ediacaran Sete Lagoas Formation, Bambuí Group, Southeast Brazil: taxonomic and biostratigraphic analyses

Matheus Denezine,[1,2]* Dermeval Aparecido do Carmo,[1] Shuhai Xiao,[2] Qing Tang,[3] Vladmir Sergeev,[4,†] Alysson Fernandes Mazoni,[5] and Carolina Zabini[5]

[1]Institute of Geosciences, University of Brasília, Brasília, Federal District 73105-909, Brazil <matheusdenezine@yahoo.com.br>, <derme@unb.br>
[2]Department of Earth Sciences, Virginia Tech, Blacksburg, Virginia 24061, USA <xiao@vt.edu>
[3]School of Earth Sciences and Engineering, Nanjing University, Nanjing 210023, China <qingt@nju.edu.cn>
[4]Geological Institute, Russian Academy of Sciences, Pyzhevskii per. 7, Moscow, 119017 Russia
[5]Institute of Geosciences, University of Campinas, Campinas, São Paulo 13083-855, Brazil <alysson.mazoni@gmail.com>, <cazabini@unicamp.br>

Non-technical Summary.—Seven species occur in shallow-marine limestone of the Sete Lagoas Formation, Bambuí Group, in Januária, Brazil, including *Siphonophycus robustum*, *Leiosphaeridia crassa*, *Leiosphaeridia jacutica*, *Leiosphaeridia minutissima*, *Leiosphaeridia tenuissima*, *Germinosphaera bispinosa*, and a new species named *Ghoshia januarensis*. In the lower part of the studied section, these occurrences are common, but only *Ghoshia januarensis* is found in the upper part. This is likely due to changes in the environment or preservation conditions. The *Leiosphaeridia* species, especially *Leiosphaeridia minutissima*, dominates the assemblage of organic-walled microfossils. While most described taxa have long stratigraphic ranges, they are consistent with a terminal Ediacaran age, as indicated by detrital zircon data and tubular fossils (e.g., *Cloudina* and *Corumbella*) from the Sete Lagoas Formation.

Abstract.—This work presents a detailed taxonomic study on organic-walled microfossils from the Ediacaran Sete Lagoas Formation (Bambuí Group) at the Barreiro section in the Januária area of the São Francisco basin, Brazil. Seven species are described, including *Siphonophycus robustum* (Schopf, 1968), *Ghoshia januarensis* new species, *Leiosphaeridia crassa* (Naumova, 1949), *Leiosphaeridia jacutica* (Timofeev, 1966), *Leiosphaeridia minutissima* (Naumova, 1949), *Leiosphaeridia tenuissima* Eisenack, 1958, and *Germinosphaera bispinosa* Mikhailova, 1986. These taxa are recovered for the first time in the Sete Lagoas Formation. They occur abundantly in the lower portion of the studied section, but only *Ghoshia januarensis* is present in the upper part of the studied section, probably due to environmental or taphonomic changes. *Leiosphaeridia* species, particularly *Leiosphaeridia minutissima*, dominate the organic-walled microfossil assemblage. Although most taxa described here have long stratigraphic ranges, they are consistent with a terminal Ediacaran age as inferred from detrital zircon data and tubular fossils (e.g., *Cloudina* and *Corumbella*) from the Sete Lagoas Formation.

UUID: http://zoobank.org/7f92b900-0176-4da6-93a3-fd51edb22cbf

Introduction

The present work provides an updated taxonomic description and biostratigraphic analysis of organic-walled microfossils from the Sete Lagoas Formation, Bambuí Group, from the countryside of Januária Municipality, Minas Gerais State, Brazil. The studied area is an ancient quarry area with an exposure of nearly 70 m of a continuous succession of mixed carbonate and fine-grained siliciclastic rocks. In addition, the Januária area has been the focus of the chronostratigraphic investigation of the Sete Lagoas Formation since Warren et al. (2014) reported Ediacaran tubular fossils such as *Cloudina* sp. and *Corumbella werneri* Hahn et al., 1982 from the lower Sete Lagoas Formation in the Januária area.

Several articles on organic-walled microfossils from the Sete Lagoas Formation have been previously published (Sommer, 1971; Simonetti and Fairchild, 1989, 2000; Fairchild et al., 1996, 2012; Sanchez and Fairchild, 2018), describing dozens of species from this unit (Table 1), although Sanchez and Fairchild (2018) invalidated one species, *Bambuites erichsenii* Sommer, 1971. It is important to underscore that the investigation conducted by Fairchild et al. (1996) centered on the analysis of silicified carbonaceous microfossils in petrographic thin sections from the Sete Lagoas Formation in the western portion of the São Francisco craton. Specimens illustrated by Fairchild

[†]Deceased.
*Corresponding author.

Table 1. List of microfossils from the Sete Lagoas Formation, Bambuí Group, published previously and in this study. Articles: 1 = Sommer (1971); 2 = Marchese (1974); 3 = Simonetti and Fairchild (1989); 4 = Fairchild et al. (1996); 5 = Simonetti and Fairchild (2000); 6 = Fairchild et al. (2012); 7 = Warren et al. (2014); 8 = Perrella Júnior et al. (2017); 9 = Sanchez and Fairchild (2018); 10 = Denezine et al. (2022); 11 = this study.

	Articles										
Species	1	2	3	4	5	6	7	8	9	10	11
cf. *Archaeotrichion contortum* Schopf, 1968				X							
cf. *Archaeotrichion* sp.				X							
Bambuites erichsenii Sommer, 1971	X								X		
cf. *Biocatenoides*				X							
Cloudina sp.							X	X			
Corumbella werneri Hahn et al., 1982							X				
cf. *Cyanonema inflatum* Oehler, 1977				X							
cf. *Dictyosphaera macroreticulata* Xing and Liu, 1973				X							
Eomycetopsis sp. A			X								
Eomycetopsis sp. B			X								
cf. *Eomycetopsis* sp.				X							
cf. *Eomycetopsis*				X							
Eosynechoccus medius Hofmann, 1976					X						
Eosynechococcus moorei Hofmann, 1976			X								
Gymnosolenides		X									
Germinosphaera bispinosa Mikhailova, 1986										X	X
Glenobotrydion aenigmatis Schopf, 1968			X								
cf. *Gloeodiniopsis* sp.				X							
cf. *Gloeodiniopsis magna* Nyberg and Schopf., 1984				X							
Ghoshia sp.										X	
Ghoshia januarensis new species											X
Leiosphaeridia sp. 1					X						
cf. *Leiosphaeridia* sp.				X							
Leiosphaeridia crassa (Naumova, 1949)											X
Leiosphaeridia jacutica (Timofeev, 1966)											X
Leiosphaeridia minutissima (Naumova, 1949)										X	X
Leiosphaeridia tenuissima Eisenack, 1958 (in Eisenack, 1958a)										X	X
Melanocyrillium sp.										X	
Myxococcoides cf. *M. cantabrigensis* Knoll, 1982			X								
Myxococcoides sp. A			X								
Myxococcoides sp. B			X								
cf. *Myxococcoides reticulata* Schopf, 1968				X							
cf. *Myxococcoides*				X							
cf. *Myxococcoides* sp.				X							
cf. *Myxococcoides globosa* Maithy and Shukla, 1977				X							
cf. *Oscillatoriopsis* sp.				X							
Palaeophycys sp.							X				
cf. *Rugosoopsis* sp.				X							
Siphonophycus robustum Schopf, 1968										X	X
Siphonophycus sp.			X								
cf. *Siphonophycus beltense* Horodyski, 1980				X							
cf. *Siphonophycus* sp.				X							
cf. *Siphonophycus*				X							
Trachyhystrichosphaera aimica Hermann, 1976 (in Timofeev et al., 1976)						X					

et al. (1996) were tentatively compared with seven species, alongside several taxa left under open nomenclature. This study provides a detailed taxonomic description with an analysis of the diversity, abundance, and stratigraphic occurrence of organic-walled microfossils from the Sete Lagoas Formation in the Barreiro section in the Januária area.

The remarkable diversity of organic-walled microfossils in the Ediacaran Period (Knoll, 1994; Vidal and Moczydłowska-Vidal, 1997; Huntley et al., 2006) is hypothesized to be associated with the ecological rise of animals (Peterson and Butterfield, 2005), followed by the advent of skeletonized animals as evidenced by fossil cloudinids and corumbellids (Germs, 1972; Hahn et al., 1982; Hua et al., 2005; Walde et al., 2015; Adôrno et al., 2017). The transition from the Ediacaran to the Cambrian Period is marked by a significant turnover of acritarch species (Anderson et al., 2017; Grazhdankin et al., 2020; Morais et al., 2021). The Cambrian is characterized by a diversification of acanthomorphs species compared with the sphaeromorph dominance in the late Ediacaran (Gaucher and Sprechmann, 2009). Acanthomorphic acritarchs define four acritarch assemblage zones to recognize the lower Cambrian on the East European Platform (Moczydłowska, 1991): *Asteridium tornatum–Comasphaeridium velvetum* Assemblage Zone, *Skiagia ornata–Fimbriaglomerella membranacea* Assemblage Zone, *Heliosphaeridium dissimilare–Skiagia ciliosa* Assemblage Zone, and *Volkovia dentifera–Liepaina plana* Assemblage Zone. These biostratigraphic units have been used to correlate Cambrian successions around the world (Zheng et al., 2020). Therefore, a systematic study of organic-walled microfossils from the Sete Lagoas Formation not only provides a tool for biostratigraphic correlation but also offers useful data to improve the understanding of Ediacaran evolution.

Geological setting

The Januária Municipality is located in the central part of the São Francisco craton (Fig. 1). The paleogeographic location of the São Francisco craton during the Ediacaran Period has not

https://doi.org/10.1017/jpa.2023.83 Published online by Cambridge University Press

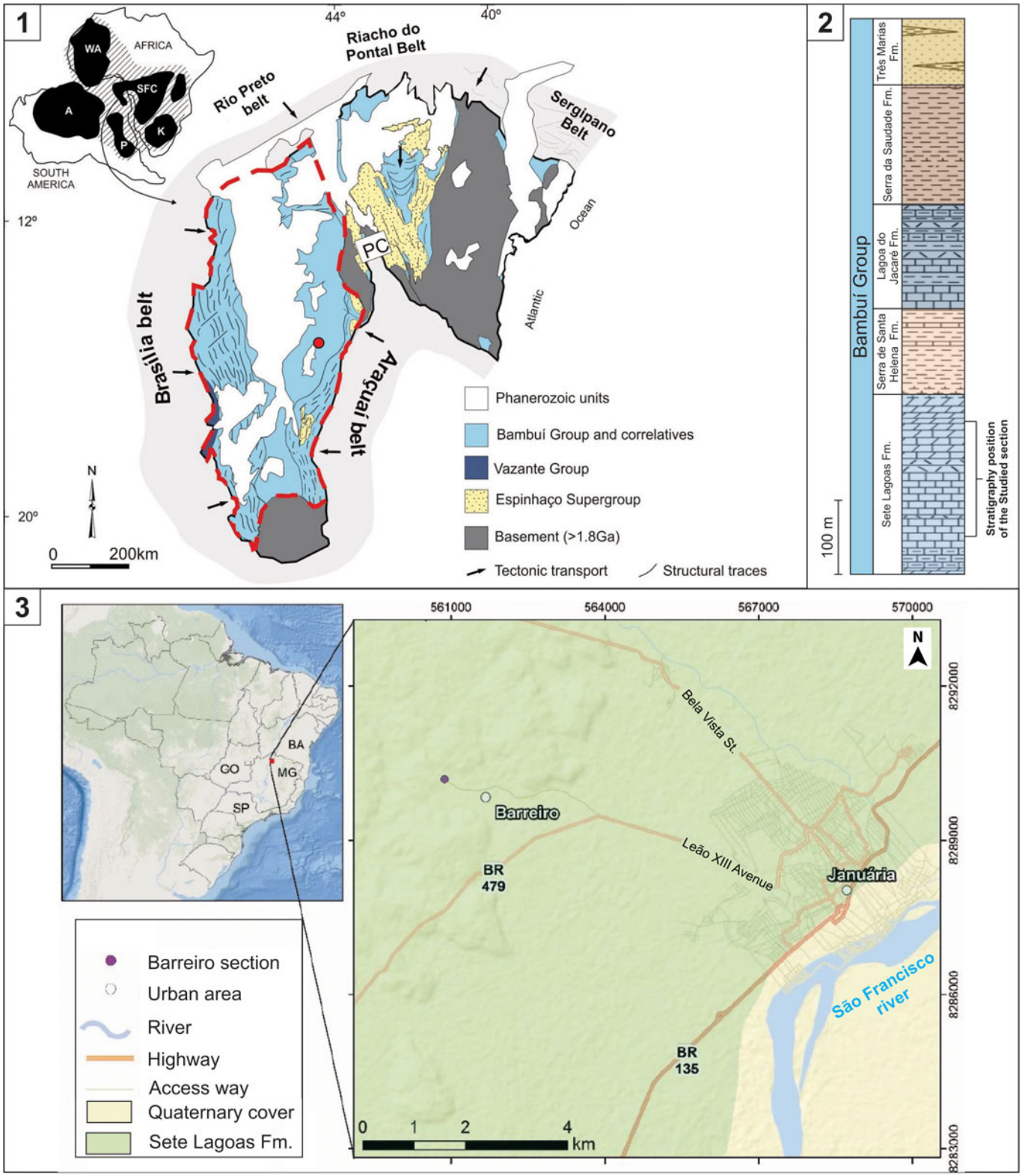

Figure 1. (**1**) Geological map of the São Francisco basin (red dashed line) in the São Francisco craton, showing its relationship with neighboring Neoproterozoic fold belts. Inset map shows major cratons in the western Gondwana in a Neoproterozoic paleogeographic configuration: A = Amazonian craton; P = Rio de la Plata craton; K = Kalahari craton; WA = West Africa craton; SFC = São Francisco-Congo craton; PC = Paramirim Corridor. Modified from Reis and Alkmim (2015). (**2**) Stratigraphic position of the studied section in the Bambui Group columnar section. (**3**) Geological map of the studied area. The purple dot marks the location of the studied section.

https://doi.org/10.1017/jpa.2023.83 Published online by Cambridge University Press

been precisely constrained, mainly because of poor biostratigraphic and paleomagnetic data. However, Merdith et al. (2021) placed the São Francisco craton in high latitudes during the Ediacaran Period.

The western portion of the São Francisco craton comprises a succession of siliciclastic and carbonate rocks dated between 1.77 Ga and 0.56 Ga (Pimentel et al., 2011; Alvarenga et al., 2012). The Brasília fold belt that bounds the western margin of the São Francisco craton was deformed during the Brasiliano–Pan African orogeny between 790 Ma and 540 Ma (Pimentel and Fuck, 1992). This fold belt borders to the east with the São Francisco craton covered with undeformed Neoproterozoic strata. It consists of a tectonic domain where only the upper 2 km strata are deformed and a domain further west where both the basement and sediment cover are deformed (Alvarenga et al., 2014). A thick interval of Mesoproterozoic and Neoproterozoic sedimentary rocks was deposited along the west portion of the São Francisco craton. These strata are separated into three stratigraphic units, including, in ascending stratigraphic order, the Paranoá Group (Barbosa, 1963), Jequitaí Formation (Oliveira and Leonardos, 1943), and Bambuí Group (Rimann, 1917).

The Sete Lagoas Formation, which is the main focus of this work, represents the basal unit of the Bambuí Group and consists of a sequence of carbonate-dominated sediments in the São Francisco basin. Those sediments are characterized by a low total organic carbon (TOC) content of less than 2% (Uhlein et al., 2019; Caetano-Filho et al., 2021) and relatively low thermal maturity (Reis and Suss, 2016). The $\delta^{13}C_{carb}$ and $\delta^{13}C_{org}$ excursions indicate a disconnection between the São Francisco basin and the global carbon cycles, which would imply marine isolation and paleogeographic shifts driven by the dynamic changes in marginal orogenic systems (Caetano-Filho et al., 2019, 2021; Guacaneme et al., 2021).

The depositional age of the Bambuí Group has long been a matter of debate. The Bambuí Group was initially considered to be Cretaceous (Liais, 1872 in Couto et al., 1981), but recent studies show that it is probably Ediacaran–Cambrian (Pimentel et al., 2011; Warren et al., 2014; Paula-Santos et al., 2015; Moreira et al., 2020; Sanchez et al., 2021; DaSilva et al., 2022). Geochronological constraints on the Bambuí Group are few and inconclusive. Carbonates of the lower Sete Lagoas Formation yielded Pb–Pb apparent ages of ~740 Ma (Babinski et al., 2007). However, Caxito et al. (2021) analyzed samples from crystal-fan-bearing limestone from the base of the Sete Lagoas Formation and obtained U–Pb ages of 615.4 ± 5.9 Ma if both the crystal fans and matrix were considered together, 608.1 ± 5.1 Ma for crystal fans, and 607.2 ± 6.2 Ma for the matrix. The youngest population of detrital zircons from the Sete Lagoas Formation gave U–Pb ages of ~557 Ma (Paula-Santos et al., 2015), and the youngest population of detrital zircons from the Três Marias Formation gave U–Pb ages of ~620 Ma (Rodrigues, 2008; Pimentel et al., 2011), providing maximum age constraints on the host strata. More recently, a zircon U–Pb age of 520.2 ± 5.3 Ma has been reported from a volcanic ash bed in the Serra da Saudade Formation (Moreira et al., 2020), suggesting that the upper Bambuí Group may belong to Stage 2 of the Cambrian System.

The possible occurrence of *Cloudina* sp. and *Corumbella werneri*—tubular fossils typically found in terminal Ediacaran rocks—in the lower Sete Lagoas Formation (Warren et al., 2014; Perrella Júnior et al., 2017) and the putative presence of *Treptichnus pedum* (Seilacher, 1955)—a trace fossil whose first appearance is used to define the base of the Cambrian System—in the Três Marias Formation (Sanchez et al., 2021) also indicate that perhaps the entire Bambuí Group is Ediacaran–Cambrian, although the conflict with the ~740 Ma Pb–Pb age from the Sete Lagoas Formation (Babinski et al., 2007) remains unresolved.

Materials and methods

The studied Barreiro section is located in the Santa Luzia quarry near the Barreiro Community, western Januária Municipality, Minas Gerais State, Brazil (Fig. 1). The samples were collected from two different mining benches, as well as exposures in the hills where the Santa Luzia quarry is located. The stratigraphic thickness of the Sete Lagoas Formation in the studied area is about 70 m (Fig. 2).

The lower 15 m of the studied section consists mainly of dark gray, laminated, microcrystalline lime mudstones with a predominance of parallel bedding with microbial mats. However, there are cross-laminations in layers of fine calcareous grainstones. Microbial mats, silicified ooids, and dolomitic nodules are common at this level (Fig. 2). Intraclastic carbonate breccias, with flat pebbles ranging from <1 to 50 cm and light gray micritic matrix are present at 16 m of the section and above, intercalated with limestones. The top of the section, at around 66 m, is composed of light gray, oolitic, crystalline dolomitic grainstones, sometimes with intraclasts. Such carbonates are cross-stratified. This dolomitic interval presents incipient flat stratification, about 2 cm thick, defined by the changes in the amount of sand-size constituents.

A total of 79 stratigraphic levels were sampled. The curatorship of the rock samples, the remaining organic residues, and the palynological slides followed the protocol presented in Denezine et al. (2022). Each residual sample was coded with the MP prefix. All specimens recovered from the Sete Lagoas Formation herein illustrated are coded with the CP prefix. Each illustrated specimen is provided with a slide number followed by England Finder coordinates.

Organic-walled microfossils were extracted from thinly laminated lime mudstones and light- to dark-gray fine-grained limestone samples using acid maceration techniques. The samples were dissolved using hydrochloric and hydrofluoric acids. Residues were rinsed repeatedly in distilled water, and after the residues were settled following each rinse, the supernatant was decanted. No centrifugation was used, to minimize mechanical damage to organic-walled microfossils. No oxidative procedure was applied on organic residues. Transmitted-light photomicrographs were acquired using an Axio Imager.A2 microscope equipped with an AxioCam MRc digital camera (both Carl Zeiss). The organic-walled microfossils were also analyzed using epifluorescence microscopy; however, no fluorescence was observed in the specimens recovered.

Size analysis of *Leiosphaeridia* specimens is based on the measurement of their vesicle diameters. Vesicle diameter, along with vesicle wall thickness, was used to identify the four

https://doi.org/10.1017/jpa.2023.83 Published online by Cambridge University Press

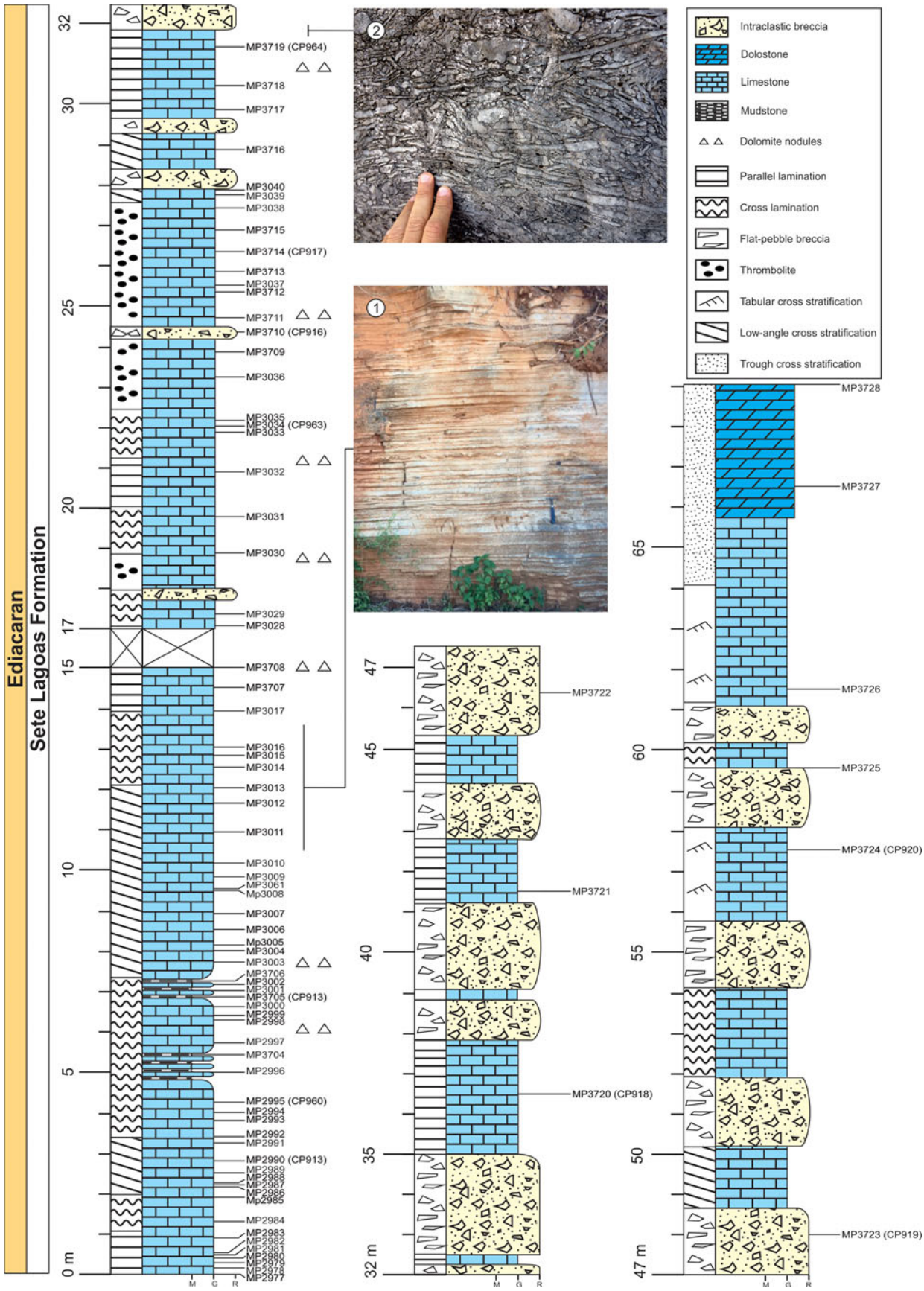

Figure 2. Stratigraphic column and field photographs of the Sete Lagoas Formation at the Barreiro section, Santa Luzia quarry, Januária Municipality, Minas Gerais State, Brazil. (**1**) Thin-bedded limestone. (**2**) Intraclastic breccia. Sample horizons are marked with the sample number prefixes MP. Sample numbers in bold mark fossiliferous horizons. The CP- numbers refer to the palynological slides of the illustrated specimens.

https://doi.org/10.1017/jpa.2023.83 Published online by Cambridge University Press

morphospecies of *Leiosphaeridia* present in the Sete Lagoas Formation: *Leiosphaeridia crassa* (Naumova, 1949), *Leiosphaeridia jacutica* (Timofeev, 1966), *Leiosphaeridia minutissima* (Naumova, 1949), and *Leiosphaeridia tenuissima* Eisenack, 1958.

Abundance data were collected in this study. All palynological slides were examined thoroughly, and complete specimens were counted. Due to their colonial nature or frequent preservation as fragments, the abundance of *Siphonophycus robustum* (Schopf, 1968) and *Ghoshia januarensis* n. sp. was not quantified.

Selected organic-walled microfossils from the Sete Lagoas Formation were analyzed using Raman spectroscopy. Specimens were placed on palynological slides and analyzed on a HORIBA JobinYvon LabRAM HR800 Raman microprobe equipped with a high-resolution 600 mm focal length spectrometer and a 514 nm argon laser source in the Department of Geosciences at Virginia Tech. The laser beam was focused to less than 10 μm in diameter with a 40× objective lens. Raman spectra were acquired using the software Labspec 5.0 with an acquisition time of less than one minute for each analysis and an excitation power of 600 mW.

Raman spectroscopy data were processed using Python modules. Baseline correction was applied to the raw data by adjusting a polynomial (third-order) curve using the Raman data from 800 and 2,100 cm^{-1} that captures the Raman peaks of carbonaceous material. After baseline correction, the four Raman peaks of carbonaceous material (i.e., D_1, D_2, D_3, D_4) were decomposed using fitting G of Kouketsu et al. (2014).

The processed Raman data were subjected to principal component analysis (PCA) in Python. The peak position, peak height, and full width at half maximum of the four Raman peaks of carbonaceous material (D_1–D_4) were used in PCA. The Python package for PCA is publicly available (Mazoni, 2021), and PCA in this study used the Python modules Numpy (Harris et al., 2020), Scipy (Virtanen et al., 2020), and Rampy (Le Rosq, 2021).

Repository and institutional abbreviation.—Types, figured specimens, and other specimens examined in this study are deposited in the Paleontological Collection under the prefix MP in the Museum of Geosciences (MGeo-UnB), University of Brasília, Brasília, Brazil.

Systematic paleontology

The suprageneric taxonomy follows the system of modern cyanobacteria and the informal classification of acritarchs (e.g., Butterfield et al., 1994; Sergeev and Schopf, 2010). Seven organic-walled microfossil species were recovered: *Ghoshia januarensis* n. sp., *Germinosphaera bispinosa* Mikhailova, 1986, *Leiosphaeridia crassa* (Naumova, 1949), *Leiosphaeridia jacutica* (Timofeev, 1966), *Leiosphaeridia minutissima* (Naumova, 1949), *Leiosphaeridia tenuissima* Eisenack, 1958, and *Siphonophycus robustum* (Schopf, 1968) (Figs. 3, 4). Two of them, *Siphonophycus robustum* and *Ghoshia januarensis*, are considered cyanobacteria. Four of them, *Leiosphaeridia crassa*, *Leiosphaeridia jacutica*, *Leiosphaeridia minutissima*, and *Leiosphaeridia tenuissima*, are sphaeromorph acritarchs traditionally regarded as protists. The phylogenetic affinity of *Germinosphaera bispinosa* is uncertain.

Kingdom Eubacteria Woese and Fox, 1977
Phylum Cyanobacteria Stanier et al., 1978
Class Hormogoneae Thuret, 1875
Order Oscillatoriales Elenkin, 1949
Family Oscillatoriaceae Kirchner, 1900
Genus *Siphonophycus* Schopf, 1968

Type species.—*Siphonophycus kestron* Schopf, 1968 (holotype: Paleobotany Collection Harvard University no. 58469, stage coordinates 33.6 × 101.4) from the black chert facies in the middle third of the late Precambrian Bitter Springs Formation, exposed on the south slope of the ridge about 1 mile north of Ross River Tourist Camp (Love's Creek Homestead), 40 miles northeast of Alice Springs, Northern Territory, Australia, by original designation.

Other species.—*Siphonophycus thulenema* Butterfield in Butterfield et al., 1994; *Siphonophycus septatum* (Schopf, 1968); *Siphonophycus robustum* (Schopf, 1968); *Siphonophycus typicum* (Hermann, 1974); *Siphonophycus kestron* Schopf, 1968; S*iphonophycus solidum* (Golub, 1979); S*iphonophycus punctatum* Maithy, 1975; and S*iphonophycus gigas* Tang et al., 2013.

Original diagnosis by Schopf (1968).—"Thallus broad, tubular, nonseptate, unbranched, commonly quite long, finely rugose in surface texture. Thallus cylindrical, somewhat tapered toward apices, solitary, straight to slightly bent, up to 180 μm long (incomplete specimen), occasionally folded and distorted. Apices apparently capitate, more-or-less constricted adjacent to expanded, broadly conical, bluntly pointed terminus. Thallus quite broad, 8.3–15.00 μm wide, commonly about 12.5 μm wide (based on five specimens), ornamented and ringed by finely punctate surficial ridges regularly spaced out 2/3 μm apart. Reproductive structures unknown."

Emended diagnosis by Knoll et al. (1991).—"Tubular, filamentous microfossils, nonseptate and unbranched, with little or no tapering toward filament termini; tubes truncated and open at ends or with closed, more or less hemispherical terminations; walls typically preserved as chagrenate to finely reticulate organic matter, but may be preserved as carbonate rinds."

Remarks.—The genus *Siphonophycus* is characterized by smooth and thin wall filaments without ornamentation. The taxon is traditionally interpreted as representing empty sheaths of filamentous cyanobacteria, but because of simple morphology, it could include a range of bacterial and eukaryotic organisms (Butterfield et al., 1994). Although it is here placed under cyanobacteria, we recognize that *Siphonophycus* is a form taxon, and several other genera of filamentous microfossils (e.g., *Eomycetopsis*, *Tenuofilum*, and *Leiotrichoides*) are regarded as synonyms of *Siphonophycus* (Knoll et al., 1991).

https://doi.org/10.1017/jpa.2023.83 Published online by Cambridge University Press

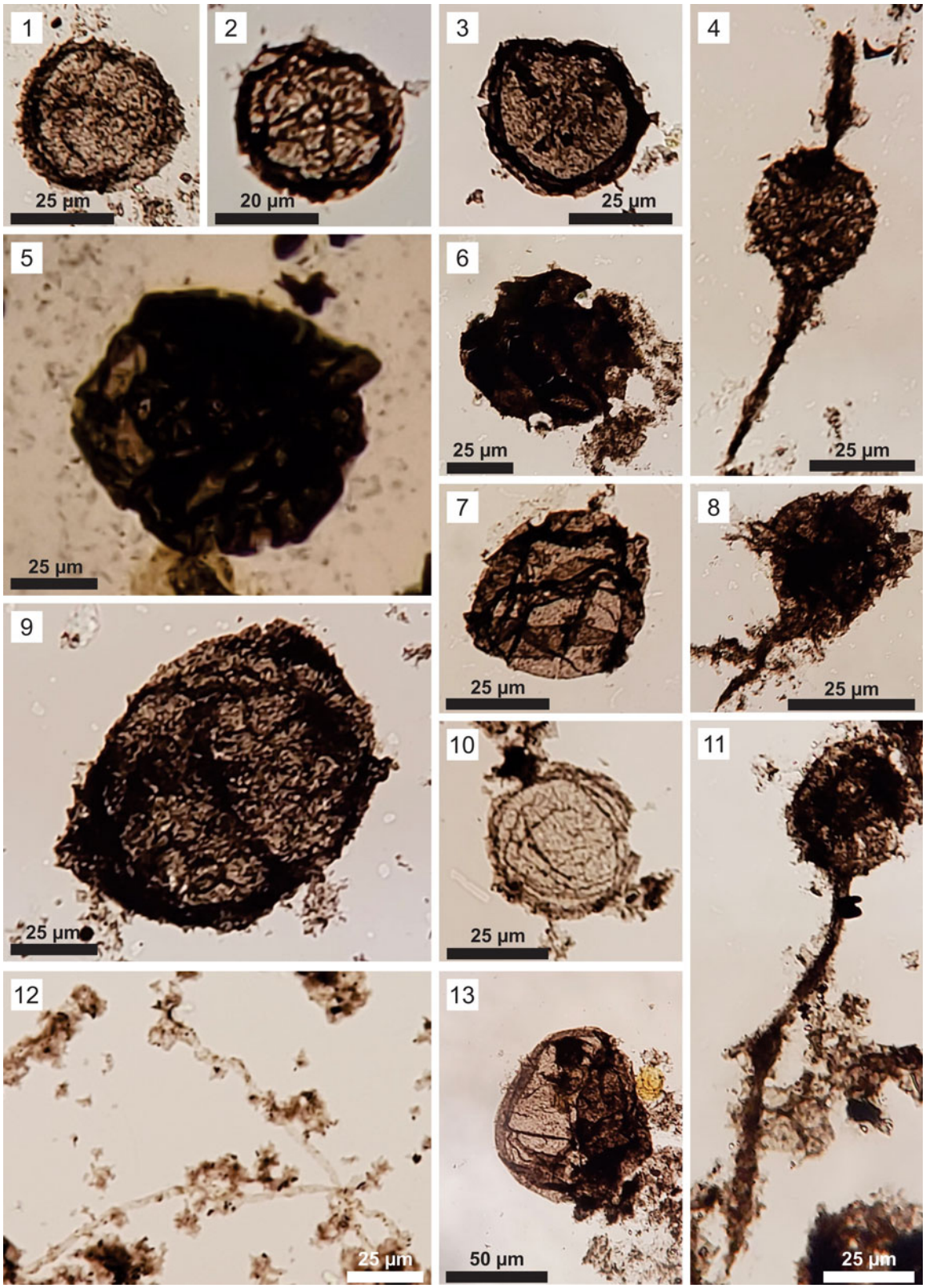

Figure 3. Organic-walled microfossils from the Sete Lagoas Formation at the Barreiro section. Slide number and England Finder coordinates (in parentheses) are given for each illustrated specimen. (**1–3, 7, 10**) *Leiosphaeridia minutissima*: (**1**) CP962 (S32); (**2**) CP962 (F48); (**3**) CP918 (K22); (**7**) CP964 (P29); (**10**) CP963 (F33). (**4, 8, 11**) *Germinosphaera bispinosa*, all in slide CP917 (EF coordinates: S26, I43, and O28, respectively). (**5**) *Leiosphaeridia jacutica*, CP913 (Y23). (**6**) *Leiosphaeridia crassa*, CP964 (H29). (**9, 13**) *Leiosphaeridia tenuissima*, all in slide CP914 (EF coordinates: Q30 and R23, respectively). (**12**) *Siphonophycus robustum*, CP960 (I50).

https://doi.org/10.1017/jpa.2023.83 Published online by Cambridge University Press

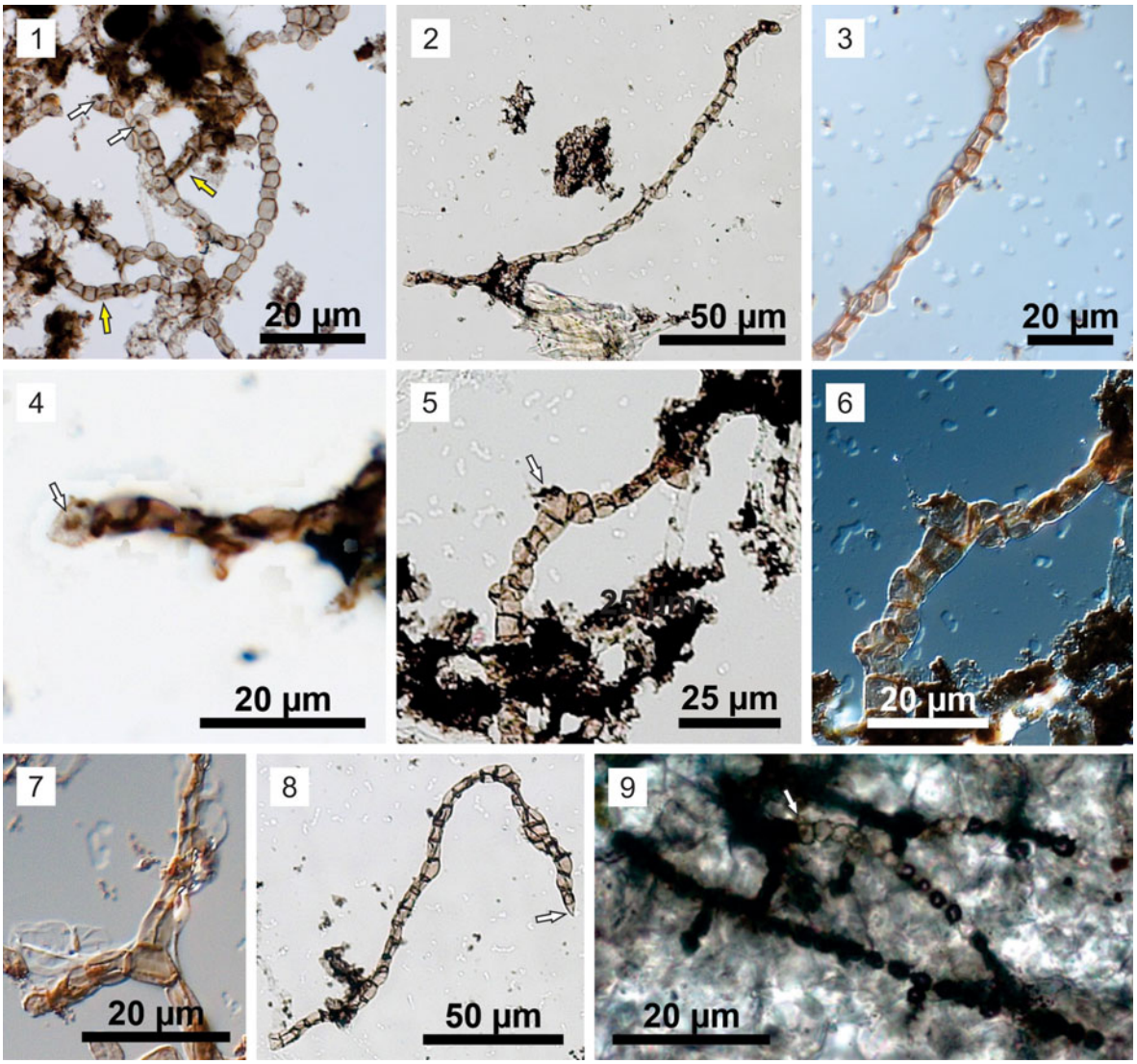

Figure 4. *Ghoshia januarensis* n. sp. from the Sete Lagoas Formation in the Barreiro section. (**1**) Holotype: CP916 (E46). Note dark spots inside cells indicated by white arrows. Yellow arrows indicate slightly deflated and deformed cells. (**2–8**) Paratypes: (**2–4**) CP919 (E18); (**3**) magnified view of the upper right part of (**2**), showing slightly deflated and deformed cells; (**4**) magnified view of the lower left part of (**2**), showing dark spot in terminal cell (arrow); (**5, 6**) CP919 (J16); (**6**) dark-field view of the central part of (**5**), showing a polyhedral cell (arrow in **5**). (**7**) CP919 (J26); note polyhedral cell at branching point. (**8**) CP920 (N18/3), showing pointed terminal cell (arrow). (**9**) Specimen identified in a petrographic thin section of the Sete Lagoas Formation at the Barreiro section in the Januária area. Reproduced from Perrella Júnior et al. (2017) with permission.

Siphonophycus robustum (Schopf, 1968) emend. Knoll et al., 1991
Figure 3.12

1968 *Eomycetopsis robusta* Schopf, p. 685, pl. 82, figs. 2, 3, pl. 83, figs. 1–4.
1968 *Eomycetopsis filiformis* Schopf, p. 685, pl. 82, figs. 1, 4, pl. 83, figs. 5–8.
1979 *Eomycetopsis robusta*; Knoll and Golubic, p.149, fig. 4a, b.
1982 *Eomycetopsis robusta*; Mendelson and Schopf, p. 59, pl. 1, figs. 9, 10.
1984 *Eomycetopsis robusta*; Sergeev, p. 436, fig. 2a–ã.
1991 *Eomycetopsis robusta*; Hofmann and Jackson, p. 367, fig. 5.1–5.3, 5.8.
1991 *Siphonophycus robustum* (Schopf, 1968); Knoll et al., p. 565, fig. 10.3, 10.5.
1992 *Eomycetopsis robusta*; Zang and Walter, p. 314, pl. 17, figs. g–I, p. 308, pl. 18, fig. g.
1992 *Eomycetopsis robusta*; Sergeev, p. 93, pl. 7, figs. 9, 10, pl. 16, figs. 3, 6, 7, 10; pl. 19, figs. 1, 5–10, pl. 24, fig. 7.
1993 *Eomycetopsis robusta*; Golovenok and Belova, pl. 2, fig. å.
1994 *Siphonophycus robustum*; Butterfield et al., p. 64, fig. 26a, g.
1994 *Siphonophycus robustum*; Hofmann and Jackson, p. 10, fig. 11.5.
1994 *Siphonophycus robustum*; Sergeev, p. 250, fig. 8f.
1994 *Siphonophycus robustum*; Sergeev et al., pl. 3, fig. 6.
1995 *Siphonophycus robustum*; Kumar and Srivastava, p. 114, fig. 14c–e.

https://doi.org/10.1017/jpa.2023.83 Published online by Cambridge University Press

1995 *Siphonophycus robustum*; Zang, p. 172, figs. 26a, 32l, m.
1997 *Siphonophycus robustum*; Sergeev et al., p. 230, fig. 14a.
1998 *Siphonophycus robustum*; Kumar and Venkatachala, p. 63, fig. 6c.
2001 *Siphonophycus robustum*; Sergeev, p. 442, fig. 7.8, 7.9.
2001 *Siphonophycus robustum*; Sergeev and Lee, p. 6, pl. 1, figs. 1, 2, 7, 11, 12.
2001 *Siphonophycus robustum*; Samuelsson and Butterfield, p. 240, figs. 2b, 9h.
2003 *Siphonophycus robustum*; Gaucher et al., fig. 6c, d.
2003 *Siphonophycus robustum*; Gaucher and Germs, fig. 7.12.
2004 *Siphonophycus robustum*; Sharma and Sergeev, figs. 3c, 4a, 6b, e, 7c, f, 9e, 11f.
2004 *Siphonophycus robustum*; Sergeev and Lee, pl. 2, fig. 4.
2004 *Siphonophycus robustum*; Tiwari and Pant, fig. 3i, n.
2005 *Siphonophycus robustum*; Prasad et al., pl. 1, fig. 7, pl. 5, fig. 12.
2006 *Siphonophycus robustum*; Sergeev, p. 213, pl. 6, figs. 9, 10, pl. 17, fig. 1, pl. 19, figs. 8, 9, pl. 22, figs. 1, 2, 7, 8, 11, 12, pl. 25, figs. 1, 3, pl. 27, figs. 4, 5, pl. 28, fig. 2, pl. 36, figs. 1, 2, pl. 44, figs. 1–7, 13, pl. 46, figs. 7–10, pl. 48, fig. 4.
2008 *Siphonophycus robustum*; Kumar and Pandey, fig. 3a, b.
2008 *Siphonophycus robustum*; Sergeev et al., pl. 6, figs. 1, 5, 6, pl. 9, figs. 1–3, 5–7.
2009 *Siphonophycus robustum*; Tiwari and Pant, fig. 6a–c.
2009 *Siphonophycus robustum*; Dong et al., p. 30, fig. 6.12.
2010 *Siphonophycus robustum*; Sergeev and Schopf, p. 387, fig. 6.4.
2012 *Siphonophycus robustum*; Sergeev et al., p. 309, pl. 21, figs. 2, 4, 8–10.
2013 *Siphonophycus robustum*; Pandey and Kumar, p. 504, fig. 4e.
2013 *Siphonophycus robustum*; Knoll et al., fig. 4c.
2013 *Siphonophycus robustum*; Tang et al., fig. 13b, m.
2014 *Siphonophycus robustum*; Babu et al., fig. 3q.
2014 *Siphonophycus robustum*; Liu et al., fig. 110.1.
2015 *Siphonophycus robustum*; Vorob'eva et al., fig. 9.14.
2015 *Siphonophycus robustum*; Tang et al., fig. 18c.
2015 *Siphonophycus robustum*; Schopf et al., p. 716, fig. 11.11.
2016 *Siphonophycus robustum*; Porter and Riedman, p. 837, fig. 16.4.
2016 *Siphonophycus robustum*; Sergeev et al., fig. 8.4.
2016 *Siphonophycus robustum*; Baludikay et al., fig. 11n.
2017 *Siphonophycus robustum*; Tang et al., fig. 8a, c, d.
2017a *Siphonophycus robustum*; Shi et al., fig. 6.3, 6.5.
2017b *Siphonophycus robustum*; Shi et al., p. 721, fig. 3e, f.
2017 *Siphonophycus robustum*; Javaux and Knoll, p. 212, fig. 5.11.
2017 *Siphonophycus robustum*; Beghin et al., pl. 3, fig. i.
2017b *Siphonophycus robustum*; Sergeev et al., p. 290, fig. 5.10, 5.11.
2019 *Siphonophycus robustum*; Li et al., fig. 15h.
2019 *Siphonophycus robustum*; Loron et al., fig. 3f.
2019 *Siphonophycus robustum*; Arrouy et al., fig. 6f.
2020 *Siphonophycus robustum*; Knoll et al., p. 6, fig. 3n, o.
2020 *Siphonophycus robustum*; Arvestål and Willman, p. 22, fig. 10f.
2020 *Siphonophycus robustum*; Shukla et al., p. 496, fig. 5e.
2021 *Siphonophycus robustum*; Miao et al., p. 17, fig. 9e.
2022 *Siphonophycus robustum*; Denezine et al., fig. 11.6.

For additional synonyms, see Butterfield et al. (1994).

Holotype.—Paleobotanical collections, Harvard University (thin section Bit. Spr. 10-1, number 58491), from Neoproterozoic Bitter Springs Formation, Amadeus Basin, Australia (Schopf, 1968, pl. 83, fig. 1).

Original diagnosis by Schopf (1968).—"Filaments commonly solitary, occasionally in groups of a few entangled filaments, rarely showing plectenchymatous organization. Lateral walls approximately1/3–3/4 μ thick, markedly coriaceous, coarsely and irregularly granular in surface texture. Filaments up to 135 μ long (incomplete filament), more-or-less regularly cylindrical with a variance in diameter of less than 0.8 μ from the widest to the most narrow portion of the filament; 2.8–4.2 μ in diameter with an average width (20 filaments measured of 3.5 μ). Septate portions of filament vary in length, commonly less than 25 μ long, with filaments commonly constricted or overlapping at the septa; overlapping portions commonly with rounded ends. Reproductive structures unknown."

Emended diagnosis by Knoll and Golubic (1979).—"Filaments cylindrical; unbranched; tubular (nonseptate); bent, sinuous and tortuous; partially flattened, circular to elliptical in cross section; intertwined to form more or less dense meshworks; long. Surface coarsely to irregularly granular in texture. Occasional cylindrical and evenly spaced inclusions, homogeneously filled with fine-grained carbonaceous matter and centrally located in the 'bore' of the tube. Filaments tubular with average diameters expressed as mean ± standard deviation 2.95 ±μm (range 2.0–4.4, n = 60). Occasional long cylindrical inclusions, 1.09 ± 0.36 μm (n = 8) in diameter, 3–4 μm long located centrally within tubular filaments."

Emended diagnosis by Knoll et al. (2020).—"A species of *Siphonophycus* with tubes 2–4 μm in cross-sectional diameter."

Occurrence in the studied section.—MP2985, MP2995, MP3040, MP3708, MP3709, and MP3710.

Illustrated specimen.—CP960 (3 μm in diameter).

Remarks.—Filamentous microfossils from the Sete Lagoas Formation are scarce and restricted to *Siphonophycus robustum* (Schopf, 1968).

Order Stigonematales Geitler, 1925
Family Capsosiracea Geitler, 1925
Genus *Ghoshia* Mandal and Maithy in Mandal et al., 1984

https://doi.org/10.1017/jpa.2023.83 Published online by Cambridge University Press

Type species.—*Ghoshia bifurcata* Mandal and Maithy in Mandal et al., 1984.

Original diagnosis presented by Mandal and Maithy in Mandal et al. (1984).—"Thallus heterotrichous, erect filaments arising from basal horizontally creeping thallus, densely packed, truly laterally branched, with cells in one or two series; sheath absent; reproduction not observed."

Ghoshia januarensis new species
Figure 4

2017 Fossil filaments consisting of aligned rounded cells, Perrella Júnior et al., p. 138. fig. 7h.
2022 *Goshia* sp.; Denezine et al., fig. 11.5.

Type specimens.—Holotype: CP916. Paratypes: CP919 and CP920. Specimens are housed in the Research Collection, Museum of Geosciences, Institute of Geosciences, University of Brasília, Federal District, Brazil.

Type locality.—Sete Lagoas Formation, Bambuí Group, Santa Luzia quarry, Municipality of Januária, Minas Gerais State, Brazil.

Type horizon.—Intraclastic breccia from the Sete Lagoas Formation, Bambuí Group. Stratigraphic level: between 31.5 and 36.4 m.

Diagnosis.—A species of *Ghoshia* characterized by spherical to doliform cells that are 3–10 µm in diameter. Cells are organized to form uniserial chains that branch irregularly.

Occurrence in the studied section.—MP2980, MP3013, MP3015, MP3040, MP3710, MP3714, MP3718, MP3723, and MP3724.

Description.—Uniserial cell chains that branch irregularly. Cells are spherical (Fig. 4.1), doliform (Fig. 4.2–4.6, 4.9), or polyhedral (Fig. 4.7), with smooth cell walls. Side branches arise more or less perpendicularly to the main branches. Cells at the branching points are often polyhedral (Fig. 4.7). Cells 3–10 µm in diameter. Deformation folds, likely resulting from compression, are present in some cells (Fig. 4.2, 4.7, 4.8).

Etymology.—In reference to the Municipality of Januária, Minas Gerais State, Brazil.

Illustrated specimens.—CP916, CP919, and CP920.

Remarks.—The Sete Lagoas specimens are somewhat similar to *Arctacellularia* German in Timofeev et al., 1976 in their uniserial filaments consisting of spherical, doliform, and polyhedral cells. However, unlike the Sete Lagoas specimens, *Arctacellularia* does not branch. The Sete Lagoas specimens are also similar to the Devonian cyanobacteria *Langiella* Croft and George, 1959, *Kidstoniella* Croft and George, 1959, and *Rhyniella* Croft and George, 1959 in having branching filaments. However, these Devonian genera can be distinguished by the presence of morphologically differentiated heterocysts and akinetes or by the presence of a sheath (Croft and George, 1959). The Sete Lagoas specimens are best placed in the genus *Ghoshia*, which is characterized by branching uniserial filaments consisting of largely undifferentiated cells. The new species proposed here, *Ghoshia januarensis*, resembles *Ghoshia bifurcata* Mandal and Maithy in Mandal et al., 1984 in cell size but differs in its more variable cell shape; *Ghoshia januarensis* has spherical, doliform, and polyhedral cells, whereas *Ghoshia bifurcata* is said to have "drum-shaped to rectangular" cells (Mandal et al., 1984). In addition, some specimens of *Ghoshia bifurcata* (including the holotype; Mandal et al., 1984, pl. 4, fig. 30) seem to have cell aggregates that are not uniserially organized.

A specimen from the Sete Lagoas Formation in the Januária area illustrated as "fossil filaments consisting of aligned rounded cells" (Perrella Júnior et al., 2017, fig. 7H) shares the same characteristics of *Ghoshia januarensis*, including uniserial and branching filaments consisting of spherical cells. Thus, this specimen is here identified as *Ghoshia januarensis*. It is important to point out that the specimen illustrated in Perrella Júnior et al. (2017) was observed in a petrographic thin section, ruling out the possibility of modern contamination.

Raman spectra of the analyzed microfossils (Fig. 5) display well-developed D_1 and D_2 bands positioned at 1,350 cm^{-1} and 1,620 cm^{-1}, respectively. These characteristics are typical of organic matter spectra (Kouketsu et al., 2014). The Raman data show that the four analyzed specimens of *Ghoshia januarensis*, including the holotype, are distinct from other organic-walled microfossils from the Sete Lagoas Formation (Fig. 5). Relative to other organic-walled microfossils from the Sete Lagoas Formation, *Ghoshia januarensis* specimens exhibit broader peaks (Fig. 5.1). PCA analysis of Raman parameters also shows that *Ghoshia januarensis* specimens are separate from other organic-walled microfossils from the Sete Lagoas Formation (Fig. 5.2). Therefore, it is possible that specimens of *Ghoshia januarensis* have different thermal history from other organic-walled microfossils in the Sete Lagoas Formation, indicating that the former could be contaminations. However, the three specimens of *Ghoshia januarensis* that were analyzed for Raman spectroscopy in Fig. 5.2 overlap with the other organic-walled microfossils largely along the second PCA axis; the difference is mainly along the primary PCA axis. A similar situation is found in the four specimens of *Leiosphaeridia minutissima* that were analyzed for Raman spectroscopy (labeled as A, B, G, and H in Fig. 5.2): they exhibit a limited range and overlap with other organic-walled microfossils from the Sete Lagoas Formation along the primary PCA axis, but two specimens (labeled A and B in Fig. 5.2) are distinct from all other specimens along the secondary PCA axis. Although subtle differences in carbonaceous material Raman characteristics could be taken as evidence for different degrees of thermal maturation (Kouketsu et al., 2014), recent studies show that such differences can result from differences in organic precursors (Qu et al., 2015; Pang et al., 2020). Considering that *Ghoshia januarensis* specimens showed no fluorescence as would modern organic contaminations, and that *Ghoshia januarensis* has been found in a petrographic thin section of the Sete Lagoas Formation (Perrella Júnior et al., 2017), we conclude

https://doi.org/10.1017/jpa.2023.83 Published online by Cambridge University Press

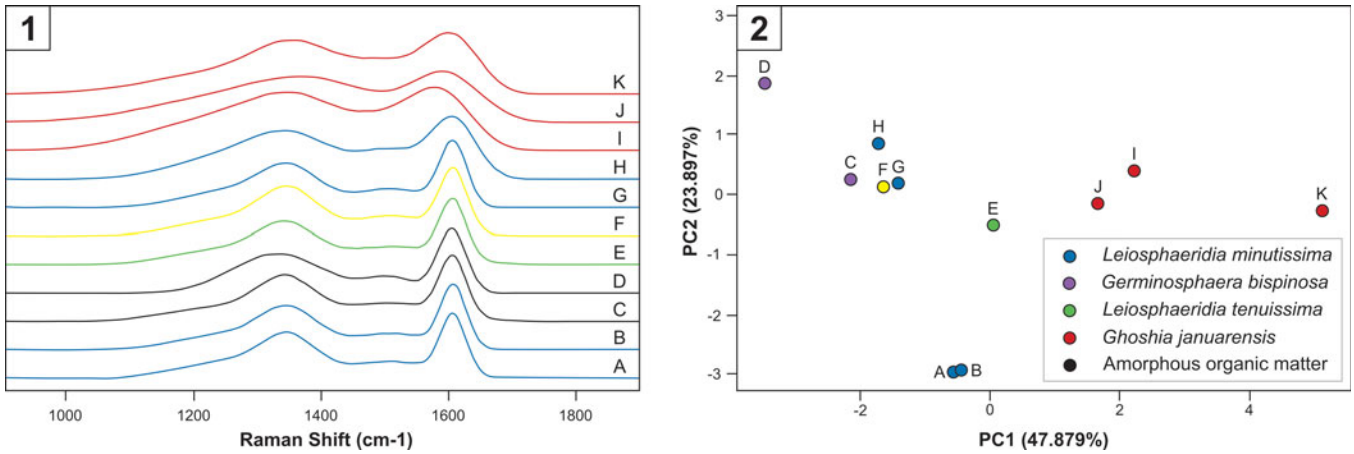

Figure 5. Raman spectroscopic data of organic-walled microfossils and amorphous organic matter from the Sete Lagoas Formation at the Barreiro section. (**1**) Baseline-corrected and fitted Raman spectra. Legends are shown in Figure 5.2. Note that Raman spectra of *Ghoshia januarensis* (J from holotype and I, K from paratypes) have broader peaks of carbonaceous matter around 1,350 cm^{-1} and 1,600 cm^{-1} relative to other Sete Lagoas organic-walled microfossils. (**2**) Principal component analysis of deconvolved Raman data. Samples: A–B and J, CP916; C–D, CP917; E, I, K, CP920; F, H, MP3728; G, MP3723.

that *Ghoshia januarensis* is indigenous to the Sete Lagoas Formation.

Group Acritarcha Evitt, 1963
Subgroup Sphaeromorphitae Downie et al., 1963
Genus *Leiosphaeridia* Eisenack, 1958

Type species.—*Leiosphaeridia baltica* Eisenack, 1958 (in Eisenack, 1958b).

Other species.—Fensome et al. (1990) revised all *Leiosphaeridia* species and listed 167 valid species.

Original diagnosis presented by Eisenack (1958b) in German.—"Hohlkugelförmige, dünnwandige und aus einer sehr widerstandsfähigen, hellgelb bis dunkelrotbraun durchscheinenden organischen Substanz bestehende Organismenreste, die oft in scheibenförmig zusammengepreßtem Zustande oder auch unregelmäßig verfaltet überliefert sein können. Wand, auch in erwachsenem Zustande, stets ohne Wandporen (Unterschied zu Tasmanites). Pylome vorhanden."

Translation of original diagnosis presented by Eisenack (1958b).—Hollow spherical, thin-walled organism residues consisting of a very resistant, light yellow to dark red-brown translucent, organic substance, which can often be preserved as a disc-shaped compressed state or an irregularly folded structure. Wall, even when fully grown, always without wall pores (in contrast to *Tasmanites*). Pylome present.

Emended diagnosis by Downie and Sarjeant (1963).—"Spherical to ellipsoidal bodies without processes, often collapsed or folded, with or without pylomes. Walls granular, punctate or unornamented, thin. Without divisions into fields and without transverse or longitudinal furrows or girdles."

Emended diagnosis by Jankauskas et al. (1989) in Russian.—"Сфероидальные оболочки с гладкой, точеечной или зеррнистой поверхиостью размером от 2–3 до 750 мкм. Толщина стенки от долей микрометра до 3–10 мкм. В ископаемом состоянии сплющены и осложнены складками смятия различной формы и размеров."

Translation of emended diagnosis by Jankauskas et al. (1989).—Spheroidal vesicle with a smooth, punctate, or granular surface ranging in size from 2–3 to 750 µm. The wall thickness varies from fractions of a micrometer to 3–10 µm. The specimens are flattened and can have compressional folds of various shapes and sizes.

Remarks.—A great number of species of the genus *Leiosphaeridia* have been reported from the Proterozoic, and many of them have very long stratigraphic ranges, e.g., from the Paleoproterozoic to the Mesozoic (Lamb et al., 2009). There are even reports of *Leiosphaeridia* species from the Miocene (Hannah et al., 2000). Because of its simple morphologies, the genus *Leiosphaeridia* is regarded as a form taxon with diverse phylogenetic affinities, and it is classified in the Acritarcha (Jankauskas et al., 1989; Grey, 2005; Sergeev and Schopf, 2010), although Sergeev and Schopf (2010) consider this taxon as belonging to the Kingdom Protista, a proposition followed here. It is important to point out that some authors relate *Leiosphaeridia* species to chlorophyceaens (Moczydlowska et al., 2011; Moczydłowska, 2016). Downie and Sarjeant (1963) emended the diagnosis of the genus *Leiosphaeridia* to exclude the reference of the vesicle color since it could reflect diagenetic features. Moreover, the maceration protocol could affect the color of organic vesicles due to the use of oxidizing solutions. Jankauskas et al. (1989) specified that the diameter of the vesicle of *Leisophaeridia* species ranges from 2–3 to 750 µm. Furthermore, Jankauskas et al. (1989) divided the smooth-walled *Leiosphaeridia* species into four species according to vesicle diameter and wall thickness, a form-taxonomical scheme followed in the present work. Butterfield et al. (1994) suggested that *Leiosphaeridia* should

https://doi.org/10.1017/jpa.2023.83 Published online by Cambridge University Press

be restricted to spheroidal fossils with vesicle walls less than 2 µm thick so that it can be differentiated from *Chuaria circularis* Walcott, 1899, which has thicker vesicle walls (2–3 µm single-wall thickness).

Leiosphaeridia crassa (Naumova, 1949) Jankauskas in Jankauskas et al., 1989
Figure 3.6

1949 *Leiotriletes crassus* Naumova, p. 54, pl. 1, figs. 5, 6, pl. 2, figs. 5, 6.
1973 *Leiopsophosphaera crassa*; Pykhova, p. 99, pl. 2, fig. 3.
1989 *Leiosphaeridia crassa* (Naumova, 1949) Jankauskas in Jankauskas et al., p. 75, pl. 9, figs. 5–10.
1992 *Leiosphaeridia crassa*; Zang and Walter, p. 289, pl. 9, figs. a–k, pl. 12, fig. k, pl. 14, figs. e, h.
1994 *Leiosphaeridia crassa*; Butterfield et al., p. 40, figs. 16f, 23k.
1994 *Leiosphaeridia crassa*; Hofmann and Jackson, p. 22, fig. 1.19–1.29.
1994 *Leiosphaeridia crassa*; Knoll, fig. 4b.
1995 *Leiosphaeridia crassa*; Zang, p. 166, figs. 21d, 28c, d.
1999 *Leiosphaeridia crassa*; Yin and Guan, p. 131, figs. 3.8, 4.5, 5.3, 5.5, 5.7, 5.11, 6.2–6.6, 6.9, 6.12.
2004 *Leiosphaeridia crassa*; Javaux et al., fig. 4e–i.
2004 *Leiosphaeridia crassa*; Sergeev and Lee, p. 21, pl. 3, figs. 4, 5.
2004 *Leiosphaeridia crassa*; Tiwari and Pant, p. 1736, fig. 3v.
2005 *Leiosphaeridia crassa*; Grey, p. 179, figs. 63a–c, 64a–d.
2005 *Leiosphaeridia crassa*; Marshall et al., fig. 1e.
2005 *Leiosphaeridia crassa*; Prasad et al., pl. 1, figs. 1, 2, pl. 4, fig. 16, pl. 5, fig. 18, pl. 9, figs. 10, 11.
2006 *Leiosphaeridia crassa*; Javaux and Marshal, fig. 3.4–3.6.
2006 *Leiosphaeridia crassa*; Sergeev and Seong-Joo, p. 15, pl. 2, figs. 2a–c, 5.
2008a *Leiosphaeridia crassa*; Moczydłowska, p. 84, figs. 7a, 8g.
2008b *Leiosphaeridia crassa*; Moczydłowska, fig. 2g.
2008 *Leiosphaeridia crassa*; Sergeev et al., pl. 7, figs. 5, 6.
2009 *Leiosphaeridia crassa*; Yin et al., figs. 3a, 3h, 3l, 4d, 4f, 4h, 5a, 5c.
2009 *Leiosphaeridia crassa*; Tiwari and Pant, figs. 7d, e, 8h, 8o, p.
2009 *Leiosphaeridia crassa*; Stanevich et al., p. 32, pl. 3, figs. 3, 4.
2010 *Leiosphaeridia crassa*; Sergeev and Schopf, p. 395, fig. 15.3–15.6.
2011 *Leiosphaeridia crassa*; Strother et al., fig. 1a, e.
2011 *Leiosphaeridia crassa*; Couëffé and Vecolii, figs. 6.2, 7.1, 7.7.
2013 *Leiosphaeridia crassa*; Tang et al., fig. 4b.
2014 *Leiosphaeridia crassa*; Lottaroli et al., fig. 10.2.
2014 *Leiosphaeridia crassa*; Babu et al., fig. 3f.
2015 *Leiosphaeridia crassa*; Tang et al., fig. 4d.
2015 *Leiosphaeridia crassa*; Nagovitsin and Kochnev, fig. 1.55, 1.56.
2016 *Leiosphaeridia crassa*; Baludikay et al., fig. 8a–c.
2016 *Leiosphaeridia crassa*; Porter and Riedman, p. 833, fig. 13.2, 13.6.
2016 *Leiosphaeridia crassa*; Sergeev et al., fig. 4.2.
2017 *Leiosphaeridia crassa*; Javaux and Knoll, p. 209, fig. 4.6.
2017 *Leiosphaeridia crassa*; Agic et al., p. 110, fig. 8a–c.
2017a *Leiosphaeridia crassa*; Sergeev et al., fig. 3.14.
2017b *Leiosphaeridia crassa*; Sergeev et al., pl. I, fig. 6.
2017 *Leiosphaeridia crassa*; Beghin et al., pl. 2, figs. c, d.
2017 *Leiosphaeridia crassa*; Suslova et al., fig. 3.1–3.4.
2019 *Leiosphaeridia crassa*; Anderson et al., p. 510, fig. 8a–e.
2018 *Leiosphaeridia crassa*; Riedman et al., fig. 5.15.
2019 *Leiosphaeridia crassa*; Arrouy et al., fig. 6d, e.
2019 *Leiosphaeridia crassa*; Li et al., fig. 4f.
2020 *Leiosphaeridia crassa*; Arvestål and Willman, p. 11, fig. 6j, k, m.
2020 *Leiosphaeridia crassa*; Knoll et al., p. 6, fig. 3g.
2020 *Leiosphaeridia crassa*; Shukla et al., p. 502, fig. 6g.
2020 *Leiosphaeridia crassa*; Pang et al., fig. 2m.

For additional synonyms, also see Jankauskas et al. (1989) and Zang and Walter (1992).

Type material.—Naumova (1949) did not designate a holotype for *Leiotriletes crassus*. Subsequently, Jankauskas in Jankauskas et al. (1989) designated one specimen of *Leiotriletes crassus* published by Naumova (1949) as a "holotype" (Naumova, 1949, pl. 1, fig. 3). In addition, he designated another specimen from a different locality and a different stratigraphic unit as a "lectotype" (Jankauskas et al., 1989, LitNIGRI, N 16-800-2942/9, specimen 2, table 9, fig. 5). By so doing, the selection of a holotype by Jankauskas can, according to the *International Code of Nomenclature for Algae, Fungi, and Plants*, be taken as the designation of a lectotype (Turland et al., 2018). In addition, the specimen designated by Jankauskas as a "lectotype" should be regarded as a neotype. According to the same code, a lectotype always takes precedence over a neotype. However, the lectotype designated by Jankauskas was a specimen of *Leiotriletes simplicissimus* (Naumova, 1949), a species he synonymized with a different species of *Leiosphaeridia*, *Leiosphaeridia minutissima*. Thus, the lectotype designated by Jankauskas is not valid, and the neotype designated by Jankauskas in Jankauskas et al. (1989) is here considered the valid type specimen of *Leiosphaeridia crassa*.

Original diagnosis presented by Naumova (1949) in Russian.—"В очертании спора округлой или округло-овальной формы. Поверхность экзины гладкая, экзина очень толстая и плотная. Форма имеет складки смятия, щель разверзания, простая. Широко распространена в нижнем кембрии Прибалтики."

Translation of original diagnosis presented by Naumova (1949).—In outline, the spore is round or round–oval. The surface of the exine is smooth, very thick, and dense. The form has compressional folds, an opening gap, and is simple. Widespread in the lower Cambrian of the Baltic.

Emended diagnosis by Javaux and Knoll (2017) and Knoll et al. (2020).—"A species of *Leiosphaeridia* with smooth, pliant walls with lanceolate folds and a modal diameter of less than 70 µm."

https://doi.org/10.1017/jpa.2023.83 Published online by Cambridge University Press

Occurrence in the studied section.—Fourteen specimens were recovered. They range from ~18 to ~62 µm in diameter: MP3719 and MP3720.

Illustrated specimen.—CP964 (diameter ~27 µm).

Remarks.—*Leiotriletes crassus* Naumova, 1949 was originally published with only a description, without a diagnosis. Although the *International Code of Nomenclature for Algae, Fungi, and Plants* states that either a description or a diagnosis is sufficient for the valid publication of a name (Turland et al., 2018, Art. 38.1), it is strongly recommended that both the diagnosis and description be presented when describing a new species (Hassemer et al., 2020). Later, Jankauskas in Jankauskas et al. (1989) reviewed some species of *Leiosphaeridia* and transferred *Leiotriletes crassus* Naumova, 1949 to the genus *Leiosphaeridia*. When *Leiotriletes crassus* was transferred to the genus *Leiosphaerida*, the species epithet was changed to *crassa,* so the gender of the epithet agrees with the gender of the genus name. Thus, this species became *Leiosphaeridia crassa* (Naumova, 1949) Jankauskas in Jankauskas et al., 1989. In addition, Jankauskas et al. (1989) did not include in their synonym list the species *Leiopsophosphaera crassa* Pykhova, 1973. Finally, Fensome et al. (1990), also in a work of taxonomic revision, transferred *Leiopsophosphaera crassa* Pykhova, 1973 to *Leiosphaeridia crassa* (Pykhova, 1973). However, Fensome et al. (1990) did not consider the study of Jankauskas et al. (1989) and regarded *Leiotriletes crassus* Naumova, 1949 as taxonomically uncertain (Grey, 2005). Thus, *Leiosphaeridia crassa* (Pykhova, 1973) is a junior homonym of *Leiosphaeridia crassa* (Naumova, 1949) Jankauskas in Jankauskas et al., 1989. Nonetheless, *Leiopsophosphaera crassa* Pykhova, 1973 is considered by several authors (Yin and Guan, 1999; Grey, 2005) as a synonym of *Leiosphaeridia crassa* (Naumova, 1949), a synonymy followed in this study. *Leiosphaeridia crassa* differs from *Leiosphaeridia minutissima* in its thicker vesicle wall, and it differs from *Leiosphaeridia tenuissima* and *Leiosphaeridia jacutica* in vesicle size (Jankauskas et al., 1989).

Leiosphaeridia jacutica (Timofeev, 1966) Mikhailova and Jankauskas in Jankauskas et al., 1989
Figure 3.5

1966 *Kildinella jacutica* Timofeev, p. 30, pl. 7, fig. 2, pl.19, fig 9, pl. 61, fig. 5, pl. 67, fig. 8, pl. 72, fig. 1.
1989 *Leiosphaeridia jacutica* (Timofeev, 1966) Mikhailova and Jankauskas in Jankauskas et al., p. 77, pl. 12, figs. 3, 7, 9.
1992 *Leiosphaeridia jacutica*; Butterfield and Chandler, fig. 5e.
1994 *Leiosphaeridia jacutica*; Butterfield et al., p. 42, fig. 16h.
1994 *Leiosphaeridia jacutica*; Hofmann and Jackson, p. 22, fig. 17.1–17.4.
1995 *Leiosphaeridia jacutica*; Kumar and Srivastava, p. 106, fig. 11k.
2001 *Leiosphaeridia jacutica*; Sergeev, p. 444, fig. 8.7–8.10.
2004 *Leiosphaeridia jacutica*; Javaux et al., fig. 4a–d, 4m.
2005 *Leiosphaeridia jacutica*; Grey, p. 183, fig. 63g.
2005 *Leiosphaeridia jacutica*; Marshall et al., fig. 1c.
2005 *Leiosphaeridia jacutica*; Prasad et al., pl. 3, figs. 13, 14, pl. 4, fig. 12, pl. 9, fig. 25, pl. 10, fig. 6.
2006 *Leiosphaeridia jacutica*; Sergeev and Seong-Joo, p. 14, pl. 2, fig. 6.
2006 *Leiosphaeridia jacutica*; Javaux and Marshal, fig. 3.1–3.3.
2009 *Leiosphaeridia jacutica*; Stanevich et al., p. 32, pl. 3, fig. 2.
2009 *Leiosphaeridia jacutica*; Vorob'eva et al., p. 185, fig. 14.13.
2010 *Leiosphaeridia jacutica*; Nemerov et al., fig. 6.8, 6.9.
2010 *Leiosphaeridia jacutica*; Prasad et al., pl. 1, fig. 3.
2013 *Leiosphaeridia jacutica*; Tang et al., fig. 4d.
2014 *Leiosphaeridia jacutica*; Babu et al., fig. 3l.
2015 *Leiosphaeridia jacutica*; Chiglino et al., p. 643, fig. 5b.
2015 *Leiosphaeridia jacutica*; Tang et al., figs. 4f, g, 5a.
2015 *Leiosphaeridia jacutica*; Nagovitsin and Kochnev, fig. 4.43.
2015 *Leiosphaeridia jacutica*; Vorob'eva et al., fig. 7.6.
2016 *Leiosphaeridia jacutica*; Baludikay et al., fig. 8d.
2016 *Leiosphaeridia jacutica*; Porter and Riedman, p. 833, fig. 13.3.
2016 *Leiosphaeridia jacutica*; Sergeev et al., fig. 4.1, 4.6, 4.7.
2016 *Leiosphaeridia jacutica*; Singh and Sharma, p. 80, pl. 1, figs. 9, 10.
2017 *Leiosphaeridia jacutica*; Javaux and Knoll, p. 209, fig. 4.4, 4.5.
2017a *Leiosphaeridia jacutica*; Sergeev et al., fig. 3.1, 3.9–3.11.
2017b *Leiosphaeridia jacutica*; Sergeev et al., pl. I, fig. 5.
2017 *Leiosphaeridia jacutica*; Beghin et al., pl. 2, fig. e.
2017 *Leiosphaeridia crassa*; Tang et al., fig. 3c.
2017 *Leiosphaeridia jacutica*; Tang et al., fig. 3d.
2019 *Leiosphaeridia jacutica*; Anderson et al., p. 12, fig. 8f–k.
2019 *Leiosphaeridia jacutica*; Arrouy et al., fig. 6b, c.
2019 *Leiosphaeridia jacutica*; Li et al., fig. 4h.
2020 *Leiosphaeridia jacutica*; Arvestål and Willman, p. 11, fig. 6i, 6l.
2020 *Leiosphaeridia jacutica*; Knoll et al., p. 6, fig. 2g.
2020 *Leiosphaeridia jacutica*; Shukla et al., p. 502, fig. 6l.
2020 *Leiosphaeridia jacutica*; Pang et al., fig. 2f.
2021 *Leiosphaeridia jacutica*; Han et al., fig. 3a–d.

Holotype.—IGD Russian Academy of Sciences no. 451/1, from upper Riphean, Lakhanda Group, Neryuen Formation, Siberia (Timofeev, 1966, pl. 7, fig. 2).

Diagnosis by Javaux and Knoll (2017) and Knoll et al. (2020).—"A species of *Leiosphaeridia* characterized by smooth, pliant walls with lanceolate folds and a modal diameter greater than 70 µm."

Occurrence in studied section.—Four specimens were recovered. They range from ~74 to ~98 µm in diameter: MP2990, MP3719, and MP3714.

https://doi.org/10.1017/jpa.2023.83 Published online by Cambridge University Press

Original description by Timofeev (1966) in Russian.—"Оболочки диаметром 150–250 мк, сферические, толстые, однослойные, с поверхностью от гладкой до грубошагреневой, с резко очерченными, крупными, серповидными, иногда угловатымц складками. Цвет темно-желтый, желто-коричневый."

Translation of original description by Timofeev (1966).—The vesicles are 150–250 microns in diameter, spherical, thick, single-layered, with a smooth to coarse shagreen surface that bears sharply defined, large, crescent-shaped, sometimes angular folds. Color dark yellow, yellow-brown.

Illustrated specimen.—CP913 (diameter ~81 µm).

Remarks.—Timofeev (1966) described the new species *Kildinella jacutica* Timofeev, 1966 and designated a holotype with the description of this species, but no diagnosis was provided. Later, Mikhailova and Jankauskas in Jankauskas et al. (1989) proposed that *Kildinella jacutica* should be transferred to *Leiosphaeridia jacutica* (Timofeev, 1966). They also designated a neotype for *Leiosphaeridia jacutica*. This neotype is not valid since Timofeev (1966) had designated a holotype in its publication, and there is no report of the loss of this holotype. *Leiosphaeridia jacutica* differs only by the larger size compared with *Leiosphaeridia crassa* (Jankauskas et al., 1989). The specimen illustrated by Tang et al. (2017, fig. 3) may not be *Leiosphaeridia crassa* but *Leiosphaeridia jacutica* because its diameter is around 90 µm. *Leiosphaeridia jacutica* differs from *Bambuites erichsenii* in its sphaeromorphic vesicle without processes.

Leiosphaeridia minutissima (Naumova, 1949) Jankauskas in Jankauskas et al., 1989
Figure 3.1–3.3, 3.7, 3.10

1949 *Leiotriletes minutissimus* Naumova, p. 52, pl. 1, figs. 1, 2, pl. 2, figs. 1, 2.
1989 *Leiosphaeridia minutissima* (Naumova, 1949) Jankauskas in Jankauskas et al., p. 79, pl. 9, figs. 1–4, 11.
1992 *Leiosphaeridia minutissima*; Butterfield and Chandler, fig. 3a, i.
1994 *Leiosphaeridia minutissima*; Hofmann and Jackson, p. 21, fig. 23.9–23.15.
2003 *Leiosphaeridia minutissima*; Gaucher and Germs, fig. 6.10–6.12.
2005 *Leiosphaeridia minutissima*; Grey, p. 184, fig. 63d.
2005 *Leiosphaeridia minutissima*; Blanco and Gaucher, fig. 11b.
2005b *Leiosphaeridia minutissima*; Gaucher et al., fig. 6d.
2005 *Leiosphaeridia minutissima*; Prasad et al., pl. 9, figs. 1, 3.
2008 *Leiosphaeridia minutissima*; Gaucher et al., p. 491, fig. 3a.
2008a *Leiosphaeridia minutissima*; Moczydłowska, p. 84, fig. 8h.
2008b *Leiosphaeridia minutissima*; Moczydłowska, figs. 2f, 6d.
2010 *Leiosphaeridia minutissima*; Nemerov et al., fig. 6.7.
2011 *Leiosphaeridia minutissima*; Couëffé and Vecolii, fig. 7.3.
2013 *Leiosphaeridia minutissima*; Tang et al., fig. 4a.
2015 *Leiosphaeridia minutissima*; Chiglino et al., p. 642, fig. 5a.
2015 *Leiosphaeridia minutissima*; Tang et al., fig. 4c.
2015 *Leiosphaeridia minutissima*; Nagovitsin and Kochnev, fig. 4.57, 4.58.
2015 *Leiosphaeridia minutissima*; Schopf et al., p. 724, fig. 13.10.
2016 *Leiosphaeridia minutissima*; Baludikay et al., fig. 8e.
2016 *Leiosphaeridia minutissima*; Porter and Riedman, p. 834, fig. 13.1, 13.5.
2017 *Leiosphaeridia minutissima*; Javaux and Knoll, p. 210, fig. 4.7, 4.8.
2017a *Leiosphaeridia minutissima*; Shi et al., fig. 11.6, 11.7.
2017 *Leiosphaeridia minutissima*; Beghin et al., pl. 2, figs. g, h.
2017 *Leiosphaeridia minutissima*; Tang et al., fig. 3a.
2017 *Leiosphaeridia minutissima*; Suslova et al., fig. 3.6–3.11.
2017 *Leiosphaeridia minutissima*; Agic et al., p. 110, fig. 8g, h.
2018 *Leiosphaeridia minutissima*; Yin et al., fig. 4h, 4j, 4l.
2018 *Leiosphaeridia minutissima*; Javaux and Lepot, fig. 2e.
2019 *Leiosphaeridia minutissima*; Lei et al., fig. 3.13, 3.14.
2019 *Leiosphaeridia minutissima*; Arrouy et al., fig. 5a–g, 5j.
2019 *Leiosphaeridia minutissima*; Li et al., fig. 4e.
2019 *Leiosphaeridia minutissima*; Shang et al., p. 24, fig. 21a.
2020 *Leiosphaeridia minutissima*; Arvestål and Willman, p. 11, fig. 6c–g.
2020 *Leiosphaeridia minutissima*; Knoll et al., p. 6, fig. 2a, 2c.
2020 *Leiosphaeridia minutissima*; Shukla et al., p. 502, fig. 6e, k, m.
2020 *Leiosphaeridia minutissima*; Pang et al., fig. 2n.
2021 *Leiosphaeridia minutissima*; Loron et al., fig. 6.2.
2022 *Leiosphaeridia minutissima*; Denezine et al., fig. 11.1, 11.2.

Type material.—Naumova (1949) did not designate a holotype for *Leiotriletes minutissimus*. Afterward, Jankauskas in Jankauskas et al. (1989) designated one of the specimens published by Naumova (1949, pl. 1, fig. 1) as the "holotype". In addition, he designated another specimen from a different locality and a different stratigraphic unit as a "lectotype" (Jankauskas et al., 1989, LitNIGRI, N 16-800-2942/9, table 9, fig. 1). According to the *International Code of Nomenclature for Algae, Fungi, and Plants* (Turland et al., 2018), the "holotype" selected by Jankauskas should be regarded as a lectotype and the "lectotype" regarded as a neotype. According to the same code, a lectotype takes precedence over a neotype. Thus, the lectotype designated by Jankauskas in Jankauskas et al. (1989) (Naumova, 1949, pl. 1, fig. 1) is the valid type specimen of *Leiosphaeridia minutissima*.

Diagnosis presented by Javaux and Knoll (2017).—"A species of *Leiosphaeridia* characterized by smooth walls with sinuous folds and a modal diameter less than 70 µm."

Emended diagnosis presented by Knoll et al. (2020).—"A species of *Leiosphaeridia* characterized by thin, smooth walls with sinuous folds and a modal diameter less than 70 µm."

https://doi.org/10.1017/jpa.2023.83 Published online by Cambridge University Press

Occurrence in studied section.—A total of 359 specimens were recovered. They range from ~4.4 to ~68.2 µm in diameter: MP3719, MP2977, MP2979, MP2980, MP2983, MP2985, MP2986, MP2987, MP2988, MP2992, MP2993, MP2994, MP2995, MP2998, MP2999, MP 3002, MP 3004, MP 3005, MP 3006, MP 3007, MP 3011, MP 3012, MP 3013, MP 3015, MP 3016, MP3028, MP 3030, MP3031, MP3033, MP3034, MP3035, MP3036, MP3705, MP3707, MP3708, MP3709, MP3710, MP3712, MP3713, MP3714, MP3715, MP3716, MP3719, and MP3720.

Description presented by Naumova (1949) in Russian.—"Очертание споры округлое. Экзина очень тонкая, прозрачная, наблюдаются многочисленные складки смятия. Поверхность экзины гладкая. Щель разверзания трехлучевая, простая, плохо различимая нз-за складок смятия."

Translation of description presented by Naumova (1949).—The outline of the vesicle is round. The exine is very thin, transparent, with numerous compressional folds. The surface of the exine is smooth. The opening slit is three-beam, simple, poorly distinguishable due to the compressional folds.

Illustrated specimens.—CP918 (diameter ~32 µm), CP962 (diameters 32~ µm and ~39 µm), CP963 (diameter ~38 µm), and CP964 (diameter ~45 µm).

Remarks.—The basionym of *Leiosphaeridia minutissima* (Naumova, 1949) is *Leiotriletes minutissimus* Naumova, 1949. As for *Leiotriletes crassus*, Naumova (1949) did not present a diagnosis for this species but provided a detailed description. Subsequently, Jankauskas in Jankauskas et al. (1989) transferred this species to *Leiosphaeridia minutissima* (Naumova, 1949) without presenting a diagnosis. When *Leiotriletes minutissimus* was transferred to the genus *Leiosphaerida*, the epithet was changed to *minutissima,* so the gender of the epithet agrees with the gender of the genus name. The first formal diagnosis for *Leiosphaeridia minutissima* was presented by Javaux and Knoll (2017), emended later by Knoll et al. (2020).

Leiosphaeridia tenuissima Eisenack, 1958
Figure 3.9, 3.13

1958a *Leiosphaeridia tenuissima* Eisenack, p. 391, pl. 1, figs. 2, 3.
1958b *Leiosphaeridia tenuissima*; Eisenack, pl. 2, figs. 1, 2.
1989 *Leiosphaeridia tenuissima*; Jankauskas et al., p. 81, pl. 9, figs. 12, 13.
1994 *Leiosphaeridia tenuissima*; Butterfield et al., p. 42, fig. 16i.
1994 *Leiosphaeridia tenuissima*; Hofmann and Jackson, p. 22, fig. 15.16–15.18.
1998 *Leiosphaeridia tenuissima*; Zhang et al., p. 32, fig. 9.7.
1998 *Leiosphaeridia* spp. div.; Zhang et al., p. 32, fig. 9.8, 9.9
1999 *Leiosphaeridia tenuissima*; Turnau and Racki, p. 267, pl. 5, fig. 1.
2000 *Leiosphaeridia tenuissima*; Gaucher, p. 68, pl. 11, fig. 5.
2003 *Leiosphaeridia tenuissima*; Gaucher and Germs, fig. 6.6.
2004 *Leiosphaeridia tenuissima*; Javaux et al., fig. 4j–l.
2004 *Leiosphaeridia tenuissima*; Gaucher et al., fig. 4d.
2005a *Leiosphaeridia tenuissima*; Gaucher et al., p. 549, fig. 8g–h.
2005b *Leiosphaeridia tenuissima*; Gaucher et al., fig. 6a–b, 6e–h.
2005 *Leiosphaeridia tenuissima*; Blanco and Gaucher, fig. 11a.
2005 *Leiosphaeridia tenuissima*; Grey, p. 184, fig. 63h.
2005 *Leiosphaeridia tenuissima*; Marshall et al., fig. 1d.
2005 *Leiosphaeridia tenuissima*; Prasad et al., pl. 1, fig. 3, pl. 2, fig. 10, pl. 3, fig. 15, pl. 4, fig. 17, pl. 8, figs. 16, 17.
2006 *Leiosphaeridia tenuissima*; Gaucher and Germs, p. 207, figs. 7d, f, g, 8b–f.
2007 *Leiosphaeridia tenuissima*; Javaux, fig. 1.18, 1.19.
2008 *Leiosphaeridia tenuissima*; Gaucher et al., p. 491, fig. 3b–i.
2009 *Leiosphaeridia tenuissima*; Stanevich et al., p. 32, pl. 3, fig. 5.
2010 *Leiosphaeridia tenuissima*; Prasad et al., pl. 1, fig. 1.
2010 *Leiosphaeridia tenuissima*; Buick, fig. 1e.
2013 *Leiosphaeridia tenuissima*; Tang et al., fig. 4c.
2014 *Leiosphaeridia tenuissima*; Liu et al., fig. 101.
2014 *Leiosphaeridia tenuissima*; Vorob'eva and Petrov, fig. 6b.
2015 *Leiosphaeridia tenuissima*; Schopf et al., p. 724, fig. 13.9.
2015 *Leiosphaeridia tenuissima*; Nagovitsin and Kochnev, fig. 4.59.
2015 *Leiosphaeridia tenuissima*; Chiglino et al., p. 640, fig. 4a–c.
2015 *Leiosphaeridia tenuissima*; Tang et al., fig. 4e.
2015 *Leiosphaeridia tenuissima*; Vorob'eva et al., fig. 7.8.
2016 *Leiosphaeridia tenuissima*; Baludikay et al., fig. 8f.
2016 *Leiosphaeridia tenuissima*; Porter and Riedman, p. 834, fig. 13.4.
2016 *Leiosphaeridia tenuissima*; Sergeev et al., fig. 4.2.
2016 *Leiosphaeridia tenuissima*; Singh and Sharma, p. 81, pl. 1, figs. 12, 15.
2017 *Leiosphaeridia tenuissima*; Beghin et al., pl. 2, fig. j.
2017 *Leiosphaeridia tenuissima*; Tang et al., fig. 3b.
2017 *Leiosphaeridia tenuissima*; Agic et al., p. 112, fig. 8d, f.
2017 *Leiosphaeridia tenuissima*; Suslova et al., fig. 3.13, 3.14.
2017a *Leiosphaeridia tenuissima*; Sergeev et al., fig. 3.12.
2017a *Leiosphaeridia minutissima*; Sergeev et al., fig. 3.13.
2017b *Leiosphaeridia tenuissima*; Sergeev et al., pl. 1, figs. 7, 9.
2019 *Leiosphaeridia tenuissima*; Anderson et al., p. 512, figs. 8l, m, 15k.
2019 *Leiosphaeridia tenuissima*; Arrouy et al., figs. 6a, 7a–d.
2019 *Leiosphaeridia tenuissima*; Li et al., fig. 4g.
2019 *Leiosphaeridia tenuissima*; Tang et al., fig. 1.2–1.5.
2019 *Leiosphaeridia tenuissima*; Wan et al., fig. 4f.
2020 *Leiosphaeridia tenuissima*; Arvestål and Willman, p. 12, fig. 6a, b.
2020 *Leiosphaeridia tenuissima*; Shukla et al., p. 502, fig. 6a–d, 6f.
2020 *Leiosphaeridia tenuissima*; Pang et al., fig. 2c.
2021 *Leiosphaeridia tenuissima*; Han et al., fig. 3e.

https://doi.org/10.1017/jpa.2023.83 Published online by Cambridge University Press

2021 *Leiosphaeridia tenuissima*; Tang et al., fig. 9a.
2021 *Leiosphaeridia tenuissima*; Loron et al., fig. 6.1, 6.3.
2022 *Leiosphaeridia tenuissima*; Denezine et al., fig. 11.3.

Holotype.—Preparation A3, 3 number 4, from the Dictyonema shales of the Ordovician Baltic, Nikolskaya on the Tossna, southeast Leningrad (Eisenack, 1958a, pl. 1, fig. 2).

Original diagnosis presented by Eisenack (1958a) in Germany.—"Wand äußerst dünn und zart, glasklar durchscheinend, ohne Wandporen; nur in flachgedrücktem Zustand in Form von fast kreisrunden Scheibchen überliefert. Pylome nicht beobachtet. Ø um rd 100 µm schwankend."

Translation of original diagnosis presented by Eisenack (1958a).—Wall extremely thin and delicate, crystalline translucent, without wall pores; only preserved in the flattened state in the form of almost circular disks. Pyloma not observed. Size around 100 µ.

Emended diagnosis by Javaux and Knoll (2017).—"A species of *Leiosphaeridia* characterized by smooth walls with sinuous folds and a modal diameter (rather than maximum diameter) greater than 70 µm; the wall color is not a diagnostic criteria."

Occurrence in the studied section.—Fourteen specimens were recovered. They range from ~72 to ~126 µm in diameter: MP3002, MP3007, MP2994, MP3707, MP3709, MP3013, MP3714, MP3719, and MP3720.

Illustrated materials.—CP914 (diameters: ~81 µm in Fig. 3.9 and ~86 µm in Fig. 3.13).

Remarks.—Both *Leiosphaeridia tenuissima* Eisenack, 1958 and *Leiosphaeridia minutissima* (Naumova, 1949,) are simple sphaeromorphs and have a thin and translucent wall less than 0.5 µm thick. However, Jankauskas et al. (1989) differentiated them on the basis of vesicle size, defining specimens smaller than 70 µm in diameter as *Leiosphaeridia minutissima* and specimens larger than 70 µm as *Leiosphaeridia tenuissima*. The specimen illustrated by Sergeev et al. (2017a, fig. 3.13) as *Leiosphaeridia minutissima* is better identified as *Leiosphaeridia tenuissima* due to its greatest diameter of about 105 µm.

Subgroup Acanthomorphitae Downie et al., 1963
Genus *Germinosphaera* Mikhailova, 1986

Type species.—*Germinosphaera bispinosa* Mikhailova, 1986.

Other species.—*Germinosphaera guttaformis* Mikhailova in Jankauskas et al., 1989; *Germinosphaera alveolata* Miao et al. (2019).

Original diagnosis presented by Mikhailova (1986) in Russian.—"Оболочки округлые, округло-овальные, плотные, толстые, гладкие или шагреневые, проросшие. Отростки, которые могут ветвиться, наблюдаются на одном или двух поолюсах."

Translation of original diagnosis presented by Mikhailova (1986).—The shells are round or round-oval, dense, thick, smooth or shagreen, sprouted. Processes are observed at one or two poles.

Emended diagnosis by Butterfield et al. (1994).—"Spheroidal vesicles with 1–6 open-ended, tubular, and occasionally branched processes that communicate freely with the vesicle. Multiple processes usually restricted to a single 'equatorial' plane, but otherwise non-uniformly distributed on the vesicle."

Emended diagnosis by Miao et al. (2019).—"Vesicle spheroidal, teardrop-shaped to slightly irregular outline, having psilate or low relief sculptured alveolar wall surface and bearing a single to multiple processes. Processes are simple tubular or occasionally branching, and open-ended. Processes are distributed [irregularly] on the vesicle wall, if multiple, and may be predominantly, but not exclusively, distributed in the equatorial plane of the vesicle."

Germinosphaera bispinosa Mikhailova, 1986
Figure 3.4, 3.8, 3.11

1986 *Germinosphaera bispinosa* Mikhailova, p. 33, fig. 6.
1986 *Germinosphaera unispinosa* Mikhailova, p. 33, fig. 5.
1989 *Germinosphaera bispinosa*; Jankauskas et al., p. 142, pl. 47, fig. 2.
1989 *Germinosphaera tadasii* Weis in Jankauskas et al., p. 143, pl. 47, figs. 3–5.
1989 *Germinosphaera unispinosa* Jankauskas et al., p. 143, pl. 47, fig. 1.
1991 *Germinosphaera* sp.; Knoll et al., p. 557, fig. 19.6.
1993 *Gemmispora rudis* Yan in Yan and Liu, pl. I, figs. 6, 7.
1994 *Germinosphaera fibrilla* (Ouyang et al., 1974); Butterfield et al., p. 38, fig. 17a–h.
1994 *Germinosphaera bispinosa*; Butterfield et al., p. 38, fig. 16d, e.
1994 *Germinosphaera jankauskasii* Butterfield in Butterfield et al., p. 38, fig. 16a–c.
1995 *Germinosphaera* sp. cf. *G. unispinosa*; Zang, p. 164, fig. 26k, l.
1999 *Germinosphaera unispinosa*; Yin and Guan, p. 128, fig. 5.2, 5.4, 5.6, 5.9.
2005 *Germinosphaera bispinosa*; Prasad et al., p. 44, pl. 11, fig. 3.
2005 *Germinosphaera unispinosa*; Prasad et al., p. 44, pl. 11, figs. 1, 2.
2007 *Germinosphaera unispinosa*; Yin and Yuan, fig. 2.11.
2009 *Germinosphaera* sp.; Vorob'eva et al., p. 191, fig. 13.13–-13.15, 13.17.
2016 *Germinosphaera bispinosa*; Baludikay et al., fig. 6a–c.
2017 *Germinosphaera bispinosa*; Loron and Moczydłowska, p. 24, pl. 1, fig. 3.
2019 *Germinosphaera bispinosa*; Li et al., fig. 10c–g.
2019 *Germinosphaera bispinosa*; Loron et al., fig. 8e–f.
2019 *Germinosphaera bispinosa*; Miao et al., p. 187, fig. 5d, f.
2021 *Germinosphaera bispinosa*; Miao et al., p. 14, fig. 5d, e.
2022 *Germinosphaera bispinosa*; Denezine et al., fig. 11.4.

https://doi.org/10.1017/jpa.2023.83 Published online by Cambridge University Press

Holotype.—Number 882/2 from the Krasnoyarsk region, River Uderei; Upper Riphean, Dashkin Formation (Mikhailova, 1986, fig. 6).

Diagnosis by Butterfield in Butterfield et al. (1994).—"A species of *Germinosphaera* with psilate vesicles 13–35 μm in diameter. Processes 2.5–3.5 μm wide and, when multiple, arranged equatorially on the vesicle."

Emended diagnosis by Miao et al. (2019).—"Spheroidal to slightly elongate or irregular vesicle with one to multiple tubular processes. Vesicle wall psilate. Processes may [be] arranged irregularly or equatorially on the vesicle wall when multiple."

Occurrence in the studied section.—Twenty-three specimens were recovered: MP3036 and MP3714.

Description.—Vesicles are 23.4–34.8 μm in diameter, bearing one to two processes. When two processes are present, they are inserted at two opposing ends of the vesicle (Fig. 3.4). Processes typically taper slightly toward their distal end (Fig. 3.4, lower process, 3.8) or are more or less cylindrical (Fig. 3.11). One of the processes in the specimen illustrated in Fig. 3.4 is apparently constricted at the base. However, it is uncertain whether this constriction is a taphonomic feature related to the twisting of the process. Processes are 1–3 μm in maximum diameter and 22.6–123.0 μm in preserved length.

Illustrated material.—CP917.

Remarks.—Mikhailova (1986) established two species of *Germinosphaera*, *Germinosphaera unispinosa* and *Germinosphaera bispinosa.* Two additional species were published by Jankauskas et al. (1989), *Germinosphaera guttaformis* Mikhailova in Jankauskas et al., 1989 and *Germinosphaera tadasii* Weiss in Jankauskas et al., 1989. These species were distinguished by the number of processes and the psilate versus shagrinate nature of vesicle walls. However, Butterfield et al. (1994) considered the possibility that the processes in *Germinosphaera* represent growth structures in vegetative stages, analogous to the modern xanthophyte *Vaucheria*. As such, they emended the diagnosis of *Germinosphaera* and the diagnosis of *G. bispinosa*, and they synonymized *G. unispinosa* with *G. bispinosa*. Miao et al. (2019) further emended the diagnosis of *Germinosphaera* and considered shagrinate vesicle walls to represent taphonomic alteration. Furthermore, they noted that the vesicle diameters of different species could overlap each other. Thus, they proposed that *G. tadasii* and *G. jankauskasii*, which are characterized by shagrinate vesicle walls, were junior synonyms of *G. bispinosa*. Following Miao et al. (2019), *Germinosphaera* currently has three species: *Germinosphaera bispinosa* Mikhailova, 1986, *Germinosphaera guttaformis* Mikhailova *in* Jankauskas et al., 1989, and *Germinosphaera alveolata* Miao et al., 2019.

Species diversity and abundance

The analysis of 80 samples, 53 of which contained microfossils, yielded a modest diversity of organic-walled microfossils, including seven species of four genera: *Siphonophycus robustum* (Schopf, 1968), *Leiosphaeridia crassa* (Naumova, 1949), *Leiosphaeridia jacutica* (Timofeev, 1966), *Leiosphaeridia minutissima* (Naumova, 1949), *Leiosphaeridia tenuissima* Eisenack, 1958, G*erminosphaera bispinosa* Mikhailova, 1986, and *Ghoshia januarensis* new species. Following Butterfield et al. (1994), the four morphospecies of *Leiosphaeridia* are differentiated on the basis of their vesicle diameter and wall thickness: *Leiosphaeridia minutissima* has thin-walled vesicles less than 70 μm in diameter, *Leiosphaeridia tenuissima* has thin-walled vesicles 70–200 μm in diameter, *Leiosphaeridia crassa* has thicker-walled vesicles less than 70 μm in diameter, and *Leiosphaeridia jacutica* has thicker-walled vesicles 70–800 μm in diameter (Fig. 6). Only one species of acanthomorphs is reported, *Germinosphaera bispinosa*, a smooth vesicle with one or two unbranched processes that are either cylindrical or slightly tapered toward the distal end.

Filamentous microfossils are common in the Sete Lagoas Formation. Tubular filamentous microfossils recovered in this work are represented by the morphospecies *Siphonophycus robustum*, which is interpreted as remains of cyanobacterial sheaths. This work follows Knoll et al. (1991), Butterfield et al. (1994), and Tang et al. (2013) in distinguishing *Siphonophycus* species according to their filament diameter: *Siphonophycus thulenema*, 0.5 μm in diameter; *Siphonophycus septatum,* 1–2 μm; *Siphonophycus robustum*, 2–4 μm; *Siphonophycus typicum*, 4–8 μm; *Siphonophycus kestron,* 8–16 μm; *Siphonophycus solidum*, 16–32 μm; *Siphonophycus punctatum*, 32–64 μm; and *Siphonophycus gigas*, 64–128 μm. In addition to tubular filaments, branching filaments of uniserially chained cells from the Sete Lagoas Formation are identified as *Ghoshia januarensis* new species.

The Sete Lagoas assemblage is numerically dominated by sphaeromorphs. Nearly all fossiliferous samples contain the sphaeromorph genus *Leiosphaeridia*, and *Leioshpaeridia minutissima* is the most abundant species (Fig. 6), with 359 specimens (~93% of all *Leiosphaeridia* specimens) and 1–64 occurrences per horizon in 45 horizons (Fig. 7). By contrast, *Leiosphaeridia crassa*, *Leiosphaeridia jacutica*, *Leiosphaeridia tenussima,* and *Germinosphaera bispinosa* are rare, represented by 14, 4, 9, and 19 specimens, respectively. About 73% of acritarch specimens recovered from the Sete Lagoas Formation are <40 μm in diameter, highlighting the predominance of small organic-walled microfossils in this unit.

The organic-walled microfossil assemblage recovered in this study is taxonomically different from those of previous micropaleontological studies of the Sete Lagoas Formation (e.g., Fairchild et al., 1996; Table 1). This difference is likely related to variations in paleoenvironment, paleoecology, taphonomy, and fossil preparation techniques. Previous micropaleontological studies of the Sete Lagoas Formation were focused exclusively on cherts, particularly silicified stromatolites and microbialites. Microfossils recovered in those studies were dominated by benthic microorganisms that constructed or dwelled in microbial mats. For example, Fairchild et al. (1996) documented abundant filamentous and coccoidal microfossils (e.g., *Siphonophycus*, *Myxococcoides*, *Gloeodiniopsis*) from silicified microbialites of the Sete Lagoas Formation in the State of Goiás (their localities 20–22), more than 350 km to

https://doi.org/10.1017/jpa.2023.83 Published online by Cambridge University Press

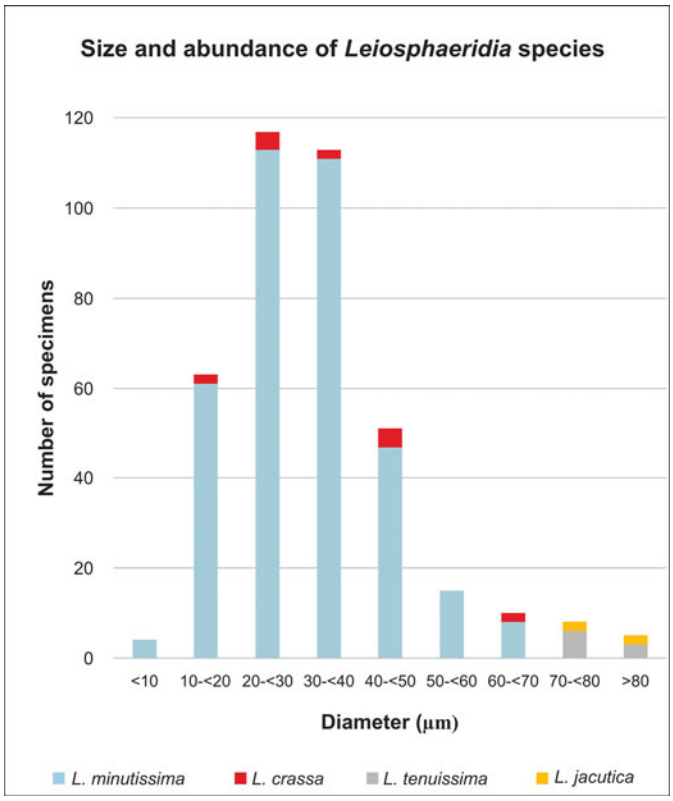

Figure 6. Abundance and size distribution of *Leiosphaeridia* species from the Sete Lagoas Formation at the Barreiro section.

the west of the Barreiro section investigated in this study; only rare acritarchs identified as cf. *Leioshpaeridia* sp. were reported (see Fairchild et al., 1996, fig, 5h, table 2). By contrast, our investigation was focused on the lime mudstone and fine-grained limestone facies dominated by planktonic microfossils such as *Leioshpaeridia minutissima*. It is well known that Precambrian chert and fine-grained siliciclastic facies tend to host taxonomically distinct microfossils, with benthic microbial mat communities dominating the former facies and planktons prevailing in the latter (Butterfield and Chandler, 1992). Thus, the taxonomic difference between this and previous studies of the Sete Lagoas Formation is likely a result of paleoenvironmental and paleoecological differences.

Taphonomic differences may also have played a role in the taxonomic difference between this and previous studies. Silicification of microfossils is fundamentally a three-dimensional cast-and-mold process at the cellular level (Xiao and Tang, 2021), whereas organic-walled microfossils in fine-grained siliciclastic facies are preserved through two-dimensional compression of recalcitrant organic structures (Butterfield, 1990), aided by clay mineral coating (e.g., Anderson et al., 2011). Thus, the taxonomic difference between chert and lime mudstone and fine-grained limestone facies of the Sete Lagoas Formation is related at least partially to taphonomic variations. However, because both paleoecological and taphonomic processes are intertwined with paleoenvironmental conditions, it is impossible to disentangle the paleoecological and taphonomic factors that may have contributed to the observed taxonomic differences.

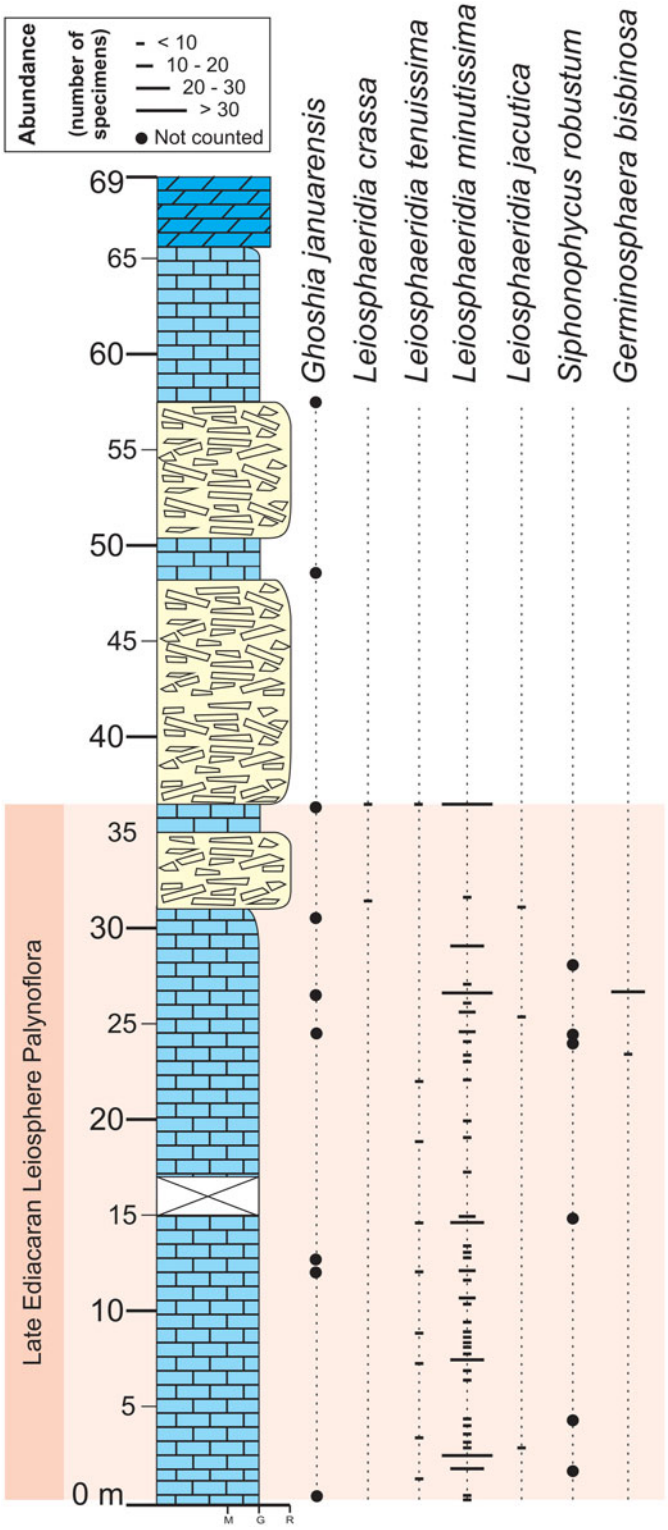

Figure 7. Stratigraphic distribution and relative abundance of organic-walled microfossils from the Sete Lagoas Formation at the Barreiro section.

Finally, methodological differences may also have played a part in the taxonomic difference between this and previous micropaleontological studies of the Sete Lagoas Formation. Organic-walled microfossils preserved in cherts are typically observed in petrographic thin sections, whereas those in fine-grained

https://doi.org/10.1017/jpa.2023.83 Published online by Cambridge University Press

siliciclastic rocks can be extracted for microscopic analysis. Such methodological difference can lead to biases in microfossil recovery and taxonomic identification, as shown in Ediacaran acritarchs (Xiao et al., 2023), which have been processed using petrographic thin sections (for those preserved three-dimensionally in cherts), hydrofluoric acid extraction (for those preserved two-dimensionally in shales), and both thin sections and acetic acid extraction (for those preserved three-dimensionally in phosphatic carbonate rocks). Therefore, the taxonomic differences between this and previous studies of the Sete Lagoas Formation likely result from a combination of paleoenvironmental, paleoecological, taphonomic, and methodological factors.

Stratigraphic distribution and biostratigraphy

Organic-walled microfossils in the Sete Lagoas Formation at the Barreiro section range from the base of the measured section to 57.5 m stratigraphic height (Fig. 7). *Ghoshia januarensis* has the greatest range of all species recovered in this work, occurring at nine stratigraphic levels from 0.4 m to 57.5 m. *Leiosphaeridia minutissima* is the longest-ranging sphaeromorph, occurring at 45 stratigraphic levels from the base of the section to 36.4 m. *Leiosphaeridia tenuissima* ranges from 1.3 to 36.4 m and is present in nine horizons, showing almost the same stratigraphic range as *Leiosphaeridia minutissima*. As a minor component of the assemblage, *Leiosphaeridia jacutica* was recovered from three levels in the interval of 2.8–31.5 m, *Leiosphaeridia crassa* from two levels in 31.5–36.4 m, *Germinosphaera bispinosa* from two horizons in 23.5–26.5 m, and *Siphonophycus robustum* from four levels in 1.9–28.0 m.

Except for *Leiosphaeridia crassa* and *Germinosphaera bispinosa,* all recovered species have their first appearance within 2 m above the base of the studied section, where there is a predominance of lime mudstone. *Leiosphaeridia crassa* and *Germinosphaera bispinosa* first emerge in the middle part of the section below the intraclastic breccia beds. The disappearance of organic-walled microfossils in the Sete Lagoas Formation is gradual, although three species (*Leiosphaeridia crassa*, *Leiosphaeridia minutissima*, and *Leiosphaeridia tenuissima*) disappear at approximately 37 m. No organic-walled microfossils other than *Ghoshia januarensis* were recovered above 37 m, right before a great abundance of intraclastic breccias, which were interpreted as seismic deposits by Okubo et al. (2020).

With the exception of *Ghoshia januarensis*, organic-walled microfossils from the Sete Lagoas Formation described in this paper have very long stratigraphic ranges when global data are considered. For example, the four *Leiosphaeridia* species recovered in this work range from the Mesoproterozoic to the Cambrian (Grey, 2005). Both *Germinosphaera bispinosa* and *Siphonopycus robustum* are known from the late Paleoproterozoic to the Paleozoic (Butterfield et al., 1994; Sergeev et al., 2012; Miao et al., 2019).

Because leiospheric sphaeromorphs have rather long stratigraphic ranges globally, they have limited utility for global biostratigraphic correlation, which casts doubt on the biostratigraphic significance of leiosphere-based biozones. Nonetheless, Grey (2005) established the Ediacaran Leiosphere Palynoflora, and Gaucher and Sprechmann (2009) proposed the Early Ediacaran Leiosphere Palynoflora. Both were regarded as early Ediacaran (ca. 635–580 Ma) acritarch biozones. More recent studies from South China, however, recovered abundant and diverse acanthomorphs from early Ediacaran strata (Zhou et al., 2007; Liu and Moczydłowska, 2019; Ouyang et al., 2021), indicating that the leiosphere-based biozones of Grey (2005) and Gaucher and Sprechmann (2009) are controlled by local environmental, regional biogeographical, or taphonomic factors.

It is perceived that the terminal Ediacaran (ca. 550–539 Ma) is characterized by a leiosphere assemblage (Knoll and Walter, 1992; Gaucher and Sprechmann, 2009) (Fig. 17). Gaucher and Sprechmann (2009) presented the Late Ediacaran Leiosphere Palynoflora, which is a low-diversity assemblage characterized by small sphaeromorphs (<150 µm) such as *Leiosphaeridia minutissima* and *Leiosphaeridia tenuissima*, among others (Fig. 17). In addition, there are occurrences of *Chuaria circularis*, as well as *Bavlinela faveolata* Shepeleva, 1962, *Soldadophycus bossii* Gaucher et al., 1996, and small acanthomorphs, such as *Asteridium* spp. The Late Ediacaran Leiosphere Palynoflora, sensu Gaucher and Sprechmann (2009), has been documented in the Nama Group in Namibia (Germs et al., 1986), the Holgat Formation of the Port Nolloth Group in Namibia (Gaucher et al., 2005a), the Mulden Group in Namibia (Gaucher and Germs, 2007), the Tent Hill Formation in Australia (Damassa and Knoll, 1986), Cijara Formation in Spain (Palacios, 1989), the Cango Caves and Gamtoos groups in South Africa (Gaucher and Germs, 2006), the Dengying Formation in South China (Yin and Yuan, 2007), the Arroyo del Soldado Group in Uruguay (Gaucher, 2000; Gaucher et al., 2003), the Sierras Bayas Group in Argentina (Cingolani et al., 1991; Gaucher et al., 2005b), the La Providencia Group in Argentina (Arrouy et al., 2019), and the Corumbá Group in Brazil (Zaine, 1991; Gaucher et al., 2003; Tobias, 2014). In Namibia, Argentina, Uruguay, and Brazil (Germs et al., 1986; Gaucher et al., 2003, 2005b; Tobias, 2014), the Late Ediacaran Leiosphere Palynoflora occurs in association with biomineralized tubular fossils such as *Cloudina lucianoi* (Beurlen and Sommer, 1957), *Cloudina riemkeae* Germs, 1972, and *Corumbella werneri* Hahn et al., 1982, which are potential index fossils for the terminal Ediacaran.

Given the predominance of a depauperate leiosphere assemblage in the Sete Lagoas Formation (this study) and the previous report of *Cloudina* and *Corumbella* from this unit (Warren et al., 2014), it is tempting to consider that the organic-walled microfossil assemblage reported in this study is correlated with the Late Ediacaran Leiosphere Palynoflora. There are, however, two caveats. First, as discussed by Xiao and Narbonne (2020), several recent studies have shown acanthomorphs as a group may extend from the lowermost Ediacaran to the terminal Ediacaran stage in Mongolia (Anderson et al., 2017, 2019) and in Siberia (Golubkova et al., 2015; but see Vorob'eva et al., 2009), to rocks considered younger than the Shuram Excursion (Ouyang et al., 2017) or even to the early Cambrian (Grazhdankin et al., 2020). Second, a systematic description of the purported *Cloudina* and *Corumbella* fossils from the Sete Lagoas Formation (Warren et al., 2014; Perrella Júnior et al., 2017) is needed to assess their species-level identification and to support their biostratigraphic significance. Nonetheless, considering the maximum age constraint of ~557 Ma provided by detrital zircons from the upper Sete Lagoas Formation (Paula-Santos et al., 2015), the organic-walled microfossil assemblage

https://doi.org/10.1017/jpa.2023.83 Published online by Cambridge University Press

reported in this paper is consistent with a terminal Ediacaran age interpretation.

Conclusions

A modest diversity of organic-walled microfossils is reported from the Sete Lagoas Formation of Bambuí Group at the Barreiro section in the Januária area of the São Francisco basin, central Brazil. Seven species are described: *Siphonophycus robustum* (Schopf, 1968), *Ghoshia januarensis* new species, *Leiosphaeridia crassa* (Naumova, 1949), *Leiosphaeridia jacutica* (Timofeev, 1966), *Leiosphaeridia minutissima* (Naumova, 1949), *Leiosphaeridia tenuissima* Eisenack, 1958, and *Germinosphaera bispinosa* Mikhailova, 1986. The first two species are considered cyanobacteria, the four *Leiosphaeridia* species are considered possible protists, and the phylogenetic affinity of *Germinosphaera bispinosa* is uncertain. All species occur in the lower part of the studied section, but only *Ghoshia januarensis* extends to the upper portion of the studied section. The assemblage is numerically dominated by *Leiosphaeridia*, with *Leiosphaeridia minutissima* being the most abundant species. The predominance of *Leiosphaeridia* indicates that the Sete Lagoas organic-walled microfossil assemblage may be correlated with the Late Ediacaran Leiosphere Palynoflora, consistent with a terminal Ediacaran age interpretation inferred from detrital zircon data, *Cloudina*, and *Corumbella* from the Sete Lagoas Formation. However, we emphasize that further investigation is needed to test this age interpretation.

Acknowledgments

We thank all institutions that participated in the development of this research: the National Council for Scientific and Technological Development (CNPq), Coordination for the Improvement of Higher Education Personnel (CAPES), Geological Survey of Brazil (CPRM), Brazilian Petroleum Corporation (PETROBRAS), National Agency of Petroleum, Gas, and Biofuels (ANP), and the University of Brasília (UnB). We thank FINATEC for assistance in administrative affairs supporting scientific projects in Brasília. We thank A.H. Giles for grammar review and the undergraduate geology students L.R.O. Gonçalve and A.S. Reis for curating samples at UnB. This study was financed in part by the Coordination for the Improvement of Higher Education Personnel—Brazil (CAPES)—Finance Code 001. S.X. acknowledges the support from the National Science Foundation (EAR-2021207). C. Z. acknowledges the support from São Paulo Research Foundation (2021/12304-0).

Declaration of competing interests

The authors declare none.

References

Adôrno, R.R., Do Carmo, D.A., Germs, G.J.B., Walde, D.H.G., Denezine, M., et al., 2017, *Cloudina lucianoi* (Beurlen & Sommer, 1957), Tamengo Formation, Ediacaran, Brazil: taxonomy analysis of stratigraphic distribution and biostratigraphy: Precambrian Research, v. 301, p. 19–35.

Agić, H., Moczydłowska, M., and Yin, L., 2017, Diversity of organic-walled microfossils from the early Mesoproterozoic Ruyang Group, North China Craton—a window into the early eukaryote evolution: Precambrian Research, v. 297, p. 101–130.

Alvarenga, C.J.S., Dardenne, M.A., Vieira, L.C., Martinho, C.T., Guimarães, E.M., Santos, R. V., and Santana, R.O., 2012, Estratigrafia da borda ocidental da Bacia do São Francisco: Boletim de Geociências Da PETROBRAS, v. 20, p. 145–164.

Alvarenga, C.J.S., Santos, R.V., Vieira, L.C., Lima, B.A.F., and Mancini, L.H., 2014, Meso-Neoproterozoic isotope stratigraphy on carbonates platforms in the Brasília belt of Brazil: Precambrian Research, v. 251, p. 164–180.

Anderson, E., Schiffbauer, J.D., and Xiao, S., 2011, Taphonomic study of Ediacaran organic-walled fossils confirms the importance of clay minerals and pyrite in Burgess Shale-type preservation: Geology, v. 39, p. 643–646.

Anderson, R.P., Macdonald, F.A., Jones, D.S., McMahon, S., and Briggs, D.E.G., 2017, Doushantuo-type microfossils from latest Ediacaran phosphorites of northern Mongolia: Geology, v. 45, p. 1079–1082.

Anderson, R.P., McMahon, S., Macdonald, F.A., Jones, D.S., and Briggs, D.E.G., 2019, Palaeobiology of latest Ediacaran phosphorites from the upper Khesen Formation, Khuvsgul Group, northern Mongolia: Journal of Systematic Palaeontology, v. 17, p. 501–532.

Arrouy, M.J., Gaucher, C., Poiré, D.G., Xiao, S., Peral, L.E.G., Warren, L. V., Bykova, N., and Quaglio, F., 2019, A new record of late Ediacaran acritarchs from La Providencia Group (Tandilia System, Argentina) and its biostratigraphical significance: Journal of South American Earth Sciences, v. 93, p. 283–293.

Arvestål, E.H.M., and Willman, S., 2020, Organic-walled microfossils in the Ediacaran of Estonia: biodiversity on the East European Platform: Precambrian Research, v. 341, n. 105626, https://doi.org/10.1016/j.precamres.2020.105626.

Babinski, M., Vieira, L.C., and Trindade, R.I.F., 2007, Direct dating of the Sete Lagoas cap carbonate (Bambuí Group, Brazil) and implications for the Neoproterozoic glacial events: Terra Nova, v. 19, p. 401–406.

Babu, R., Singh, V.K., and Mehrotra, N.C., 2014, Neoproterozoic age based on microbiotas from the Raipur Group of Baradwar Sub-basin, Chhattisgarh: Journal Geological Society of India, v. 84, p. 442–448.

Baludikay, B.K., Storme, J.Y., François, C., Baudet, D., and Javaux, E.J., 2016, A diverse and exquisitely preserved organic-walled microfossil assemblage from the Meso-Neoproterozoic Mbuji-Mayi Supergroup (Democratic Republic of Congo) and implications for Proterozoic biostratigraphy: Precambrian Research, v. 281, p. 166–184.

Barbosa, O., 1963, Geologia Econômica e Aplicada a Uma Parte Do Planalto Central: Goiânia, DNPM/PROSPEC, 70 p.

Beghin, J., Storme, J.Y., Blanpied, C., Gueneli, N., Brocks, J.J., Poulton, S.W., and Javaux, E.J., 2017, Microfossils from the late Mesoproterozoic–early Neoproterozoic Atar/El Mreïti Group, Taoudeni Basin, Mauritania, northwestern Africa: Precambrian Research, v. 291, p. 63–82.

Beurlen, K., and Sommer, F.W., 1957, Observações estratigráficas e paleontológicas sobre o calcário Corumbá: Boletim Da Divisão de Geologia e Mineralogia, v. 168, p. 1–35.

Blanco, G., and Gaucher, C., 2005, Estratigrafia, paleontologia y edad de la Formacion Las Ventanas (Neoproterozoico, Uruguay): Latin American Journal of Sedimentology and Basin Analysis, v. 12, p. 109–124.

Buick, R., 2010, Ancient acritarchs: Nature, v. 463, p. 885–886.

Butterfield, N.J., 1990, Organic preservation of non-mineralizing organisms and the taphonomy of the Burgess Shale: Paleobiology, v. 16, p. 272–286.

Butterfield, N.J., and Chandler, F.W., 1992, Palaeoenvironmental distribution of Proterozoic microfossils, with an example from the Agu Bay Formation, Baffin Island: Palaeontology, v. 35, p. 943–957.

Butterfield, N.J., Knoll, A.H., and Swett, K., 1994, Paleobiology of the Neoproterozoic Svanbergfjellet Formation, Spitsbergen: Fossils and Strata, v. 34, 84 p.

Caetano-Filho, S., Paula-Santos, G.M., Guacaneme, C., Babinski, M., Bedoya-Rueda, C., et al., 2019, Sequence stratigraphy and chemostratigraphy of an Ediacaran–Cambrian foreland-related carbonate ramp (Bambuí Group, Brazil): Precambrian Research, v. 331, n. 105365.

Caetano-Filho, S., Sansjofre, P., Ader, M., Paula-Santos, G.M., Guacaneme, C., Babinski, M., Bedoya-Rueda, C., Kuchenbecker, M., Reis, H.L.S., and Trindade, R.I.F., 2021, A large epeiric methanogenic Bambuí sea in the core of Gondwana supercontinent? Geoscience Frontiers, v. 12, p. 203–218.

Caxito, F.A., Lana, C., Frei, R., Uhlein, G.J., Sial, A.N., et al., 2021, Goldilocks at the dawn of complex life: mountains might have damaged Ediacaran–Cambrian ecosystems and prompted an early Cambrian greenhouse world: Scientific Reports, v. 11, n. 20010.

Chiglino, L., Gaucher, C., Sial, A.N., and Ferreira, V.P., 2015, Acritarchs of the Ediacaran Frecheirinha Formation, Ubajara Group, Northeastern Brazil: Anais Da Academia Brasileira de Ciências, v. 87, p. 635–649.

Cingolani, C.A., Rauscher, R., and Bonhomme, M., 1991, Grupo La Tinta (Precaámbrico y Paleozoico inferior) provinciade Buenos Aires, República Argentina. Nuevos datos geocronoloógicos y micropaleontológicos en las sedimentitas de Villa Cacique, partido de Juarez: Revista Técnica de YPFB, v. 12, p. 177–191.

https://doi.org/10.1017/jpa.2023.83 Published online by Cambridge University Press

Couëffé, R., and Vecolii, M., 2011, New sedimentological and biostratigraphic data in the Kwahu Group (Meso- to Neo-Proterozoic), southern margin of the Volta Basin, Ghana: stratigraphic constraints and implications on regional lithostratigraphic correlations: Precambrian Research, v. 189, p. 155–175.

Couto, J.G.P., Cordani, U.G., Kawashita, K., Iyer, S.S., and Moraes, N.M.P., 1981, Considerações sobre a idade do Grupo Bambuí com base em análises isotópicas de Sr e Pb: Revista Brasileira de Geociências, v. 11, p. 5–16.

Croft, W.N., and George, E.A., 1959, Blue-green algae from the Middle Devonian of Rhynie, Aberdeenshire: Bulletin of the British Museum, v. 3, p. 341–353.

Damassa, S.P., and Knoll, A.H., 1986, Micropalaeontology of the late Proterozoic Arcoona Quartzite Member of the Tent Hill Formation, Stuart Shelf, South Australia: Alcheringa, v. 10, p. 417–430.

DaSilva, L.G., Pufahl, P.K., James, N.P., Guimaraes, E.M., and Reis, C., 2022, Sequence stratigraphy and paleoenvironmental significance of the Neoproterozoic Bambui Group, Central Brazil: Precambrian Research, v. 379, n. 106710.

Denezine, M., Adôrno, R.R., Do Carmo, D.A., Guimarães, E.M., Walde, D.H.G., Alvarenga, C.J.S., Germs, G., Antonietto, L.S., Gianfranco, C.G.V.R., and Nunes Junior, O.O., 2022, Methodological development of a combined preparation for micropaleontological and sedimentological studies of samples from the Proterozoic record: Frontiers in Earth Science, v. 10, n. 810406.

Dong, L., Xiao, S., Shen, B., Zhou, C., Li, G., and Yao, J., 2009, Basal Cambrian microfossils from the Yangtze Gorges area (South China) and the Aksu area (Tarim block, northwestern China): Journal of Paleontology, v. 83, p. 30–44.

Downie, C., and Sarjeant, W.A.S., 1963, On the interpretation and status of some hystrichosphere genera: Palaeontology, v. 6, p. 83–96.

Downie, C., Evitt, W.R., and Sarjeant, W.A.S., 1963, Dinoflagellates, hystrichospheres and the classification of the acritarchs: Geological Sciences, v. 7, 16 p.

Eisenack, A., 1958a, Microfossilien aus dem Ordovizium des Baltikums, 1, Markasitschicht, Dictyonema-Scheifer, Glaukonitsand, Glaukonitkalk: Senckenbergian Lethaea, v. 39, p. 389–404.

Eisenack, A., 1958b, *Tasmanites* Newton 1875 und *Leiosphaeridia* n. g. als Gattungen der Hystrichosphaeridea: Palaeontographica, v. 110, p. 1–19.

Elenkin, A.A., 1949, (Monographie Algarum Cyanophycearum Aquidulcium et Terrestrium Infinibus URSS Inventarum: Special Part 2): Moscos, Izd. Akademia Nauk SSSR, p. 985–1908. [in Russian]

Evitt, W.R., 1963, A discussion and proposals concerning fossil dinoflagellates, hystrichospheres, and acritarchs: Geology, v. 49, p. 158–164.

Fairchild, T.R., Schopf, J.W., Shen-Miller, J., Guimarães, E.M., Edwards, M.D., Lagstein, A., Li, X., Pabst, M., and Melo Filho, L.S., 1996, Recent discoveries of Proterozoic microfossils in south-central Brazil: Precambrian Research, v. 80, p. 125–152.

Fairchild, T.R., Sanchez, E.A.M., Pacheco, M.L.A.F., and Leme, J.M., 2012, Evolution of Precambrian life in the Brazilian geological record: International Journal of Astrobiology, v. 11, p. 309–323.

Fensome, R.A., Williams, G.L., Bars, M.S., Freeman, J.M., and Hill, J.M., 1990, Acritarchs and Fossil Prasinophytes: An Index to Genera, Species and Intraspecific Taxa: American Association of Stratigraphic Palynologist Foundation Contributions, 771 p.

Gaucher, C., 2000, Sedimentology, Palaeontology and Stratigraphy of the Arroyo Del Soldado Group (Vendian to Cambrian, Uruguay): Würzburg, Beringeria, 120 p.

Gaucher, C., and Germs, G.J.B., 2003, Preliminary biostratigraphic correlation of the Arroyo Del Soldado Group (Vendian to Cambrian, Uruguay) with the Cango Caves and Nama Groups (South Africa and Namibia): Revista de La Sociedad Uruguaya de Geología, v. 1, p. 141–160.

Gaucher, C., and Germs, G.J.B., 2006, Recent advances in South African Neoproterozoic–early Palaeozoic biostratigraphy: correlation of the Cango Caves and Gamtoos Groups and acritarchs of the Sardinia Bay Formation, Saldania Belt: South African Journal of Geology, v. 109, p. 193–214.

Gaucher, C., and Germs, G.J.B., 2007, First report of organic-walled microfossils from the Otavi and Mulden groups (Neoproterozoic, Namibia): III Symposium on Neoproterozoic–Early Palaeozoic Events in Southwestern Gondwana, p. 13–17.

Gaucher, C., and Sprechmann, P., 2009, Neoproterozoic acritarch evolution: Developments in Precambrian Geology, v. 16, p. 319–326.

Gaucher, C., Sprechmann, P., and Schipilov, A., 1996, Upper and middle Proterozoic fossiliferous sedimentary sequences of the Nico Pérez Terrane of Uruguay: lithostratigraphic units, paleontology, depositional environments, and correlations: Neues Jahrbuch für Geologie und Paläontologie, v. 199, p. 339–367.

Gaucher, C., Boggiani, P.C., Sprechmann, P., Sial, A.N., and Fairchild, T.R., 2003, Integrated correlation of the Vendian to Cambrian Arroyo del Soldado and Corumbá Groups (Uruguay and Brazil): palaeogeographic, palaeoclimatic and palaeobiologic implications: Precambrian Research, v. 120, p. 241–278.

Gaucher, C., Chiglino, L., and Peçoits, E., 2004, Southernmost exposures of the Arroyo del Soldado Group (Vendian to Cambrian, Uruguay): palaeogeographic implications for the amalgamation of W-Gondwana: Gondwana Research, v. 7, p. 701–714.

Gaucher, C., Frimmel, H.E., and Germs, G.J.B., 2005a, Organic-walled microfossils and biostratigraphy of the upper Port Nolloth Group (Namibia): implications for latest Neoproterozoic glaciations: Geological Magazine, v. 142, p. 539–559.

Gaucher, C., Poire, D.G., Peral, L.G., and Chiglino, L., 2005b, Litoestratigrafia, Bioestratigrafia y Correlaciones De Las Sucesiones Sedimentarias Del Neoproterozoico-Cambrico Del Craton Del Rio De La Plata (Uruguay y Argentina): Latin American Journal of Sedimentology and Basin Analysis, v. 12, p. 145–160.

Gaucher, C., Chiglino, L., Blanco, G., Poiré, D., and Germs, G.J.B., 2008, Acritarchs of Las Ventanas Formation (Ediacaran, Uruguay): implications for the timing of coeval rifting and glacial events in western Gondwana: Gondwana Research, v. 13, p. 488–501.

Geitler, L., 1925, Synoptische Darstellung der Cyanophyceen in morphologischer und systematishcer Hinsicht: Beihefte Zum Botanischen Centralblatt, v. 2, p. 163–324.

Germs, G.J.B., 1972, New shelly fossils from Nama Group, South West Africa: American Journal of Science, v. 272, p. 752–761.

Germs, G.J.B., Knoll, A.H., and Vidal, G., 1986, Latest Proterozoic microfossils from the Nama Group, Namibia (South West Africa): Precambrian Research, v. 32, p. 45–62.

Golovenok, V.K., and Belova., M.Y., 1993, The microfossils in the cherts from the Riphean deposits of the Turukhansk Uplift: Stratigraphy and Geological Correlation, v. 1, p. 51–61.

Golub, I.N., 1979, A new group of problematic microfossils from Vendian deposits of the Orshan depression (Russian Platform), *in* Sokolov, B.S., ed., Paleontology of Precambrian and Early Cambrian: Leningrad, Nauka, p. 147–155.

Golubkova, E.Y., Zaitseva, T.S., Kuznetsov, A.B., Dovzhikova, E.G., and Maslov, A. V., 2015, Microfossils and Rb–Sr age of glauconite in the key section of the upper Proterozoic of the northeastern part of the Russian plate (Keltmen-1 borehole): Doklady Earth Sciences, v. 462, p. 547–551.

Grazhdankin, D., Nagovitsin, K., Golubkova, E., Karlova, G., Kochnev, B., Rogov, V., and Marusin, V., 2020, Doushantuo–Pertatataka-type acanthomorphs and Ediacaran ecosystem stability: Geology, v. 48, p. 708–712.

Grey, K., 2005, Ediacaran Palynology of Australia: Memoir 31 of the Association of Australasian Palaeontologists, 439 p.

Guacaneme, C., Babinski, M., Bedoya–Rueda, C., Paula–Santos, G. M., Caetano–Filho, S., Kuchenbecker, M., Reis, H.L.S., and Trindade, R.I.F., 2021. Tectonically–induced strontium isotope changes in ancient restricted seas: the case of the Ediacaran–Cambrian Bambuí foreland basin system, east Brazil: Gondwana Research, v. 93, p. 275–290, https://doi.org/10.1016/j.gr.2021.02.007.

Hahn, G., Hahn, R., Leonardos, O.H., Pflug, H.D., and Walde, D.H.G., 1982, Körperlich erhaltene Scyphozoen-Reste aus dem Jungpräkambrium Brasiliens: Geologica et Palaeontologica, v. 16, p. 1–18.

Han, C.-M., Chen, L., Li, G.J., Pang, K., Wang, W., et al., 2021, First record of organic-walled microfossils from the Tonian Shiwangzhuang Formation of the Tumen Group in western Shandong, North China: Palaeoworld, v. 30, p. 208–219.

Hannah, M.J., Wilson, G.S., and Wrenn, J., 2000, Oligocene and Miocene marine palynomorphs from CRP-2/2A, Victoria Land Basin, Antarctica: Terra Antarctica, v. 7, p. 503–511.

Harris, C.R., Millman, K.J., van der Walt, S.J., Gommers, R., Virtanen, P., et al., 2020, Array programming with NumPy: Nature, v. 585, p. 357–362.

Hassemer, G., Prado, J., and Baldini, R.M., 2020, Diagnoses and descriptions in plant taxonomy: are we making proper use of them?: Taxon, v. 69, p. 1–4.

Hermann, T.N., 1974, (Nakhodki massovykh skopleniy trikhomov v rifee), *in* Timfeev, B.V., ed., Mikrofitofossilii proterozoya i rannego paleozoya SSSR: Leningrad, Nauka, p. 6–10. [in Russian]

Hofmann, H.J., 1976, Precambrian microflora, Belcher Islands, Canada: significance and systematics: Journal of Paleontology, v. 50, p. 1040–1073.

Hofmann, H.J., and Jackson, G.D., 1991, Shelf-facies microfossils from the Uluksan Group (Proterozoic Bylot Supergroup), Baffin Island, Canada: Journal of Paleontology, v. 65, p. 361–382.

Hofmann, H.J., and Jackson, G.D., 1994, Shale-Facies Microfossils from the Proterozoic Bylot Supergroup, Baffin Island, Canada: The Paleontological Society Memoir 37, 39 p.

Horodyski, R.J., 1980, Middle Proterozoic shale-facies microbiota from the lower Belt Supergroup, Little Belt Mountains, Montana: Journal of Paleontology, v. 54, p. 649–663.

Hua, H., Chen, Z., Yuan, X., Zhang, L., and Xiao, S., 2005, Skeletogenesis and asexual reproduction in the earliest biomineralizing animal *Cloudina*: Geology, v. 33, p. 277–280.

https://doi.org/10.1017/jpa.2023.83 Published online by Cambridge University Press

Huntley, J.W., Xiao, S., and Kowalewski, M., 2006, 1.3 billion years of acritarch history: an empirical morphospace approach: Precambrian Research, v. 144, p. 52–68.
Jankauskas, T. V., Mikhailova, N.S., and German, T.N., 1989, Mikrofossilii Dokembriya SSSR [Precambrian Microfossils of the USSR]: Leningrad, Nauka, 191 p. [in Russian]
Javaux, E.J., 2007, The early eukaryotic fossil record: Advances in Experimental Medicine and Biology, v. 607, p. 1–19.
Javaux, E.J., and Knoll, A.H., 2017, Micropaleontology of the lower Mesoproterozoic Roper Group, Australia, and implications for early eukaryotic evolution: Journal of Paleontology, v. 91, p. 199–229.
Javaux, E.J., and Lepot, K., 2018, The Paleoproterozoic fossil record: implications for the evolution of the biosphere during Earth's middle-age: Earth-Science Reviews, v. 176, p. 68–86.
Javaux, E.J., and Marshal, C.P., 2006, A new approach in deciphering early protist paleobiology and evolution: combined microscopy and microchemistry of single Proterozoic acritarchs: Review of Palaeobotany and Palynology, v. 139, p. 1–15.
Javaux, E.J., Knoll, A.H., and Walter, M.R., 2004, TEM evidence for eukaryotic diversity in mid-Proterozoic oceans: Geobiology, v. 2, p. 121–132.
Kirchner, O., 1900, Shizophyceae, *in* Engler, A., and Prantl, K., eds., Die Natürlichen Pflanzenfamilien: Leipzig, I Teil, Abteilung Ia, p. 115–121.
Knoll, A.H., 1982, Microfossils from the late Precambrian Draken Conglomerate, Ny Friesland, Svalbard: Journal of Paleontology, v. 56, p. 131–162.
Knoll, A.H., 1994, Proterozoic and early Cambrian protists: evidence for accelerating evolutionary tempo: Proceedings of the National Academy of Sciences of the United States of America, v. 91, p. 6743–6750.
Knoll, A.H., and Golubic, S., 1979, Anatomy and taphonomy of a Precambrian algal stromatolite: Precambrian Research, v. 10, p. 115–151.
Knoll, A.H., and Walter, M.R., 1992, Latest Proterozoic stratigraphy and Earth history: Nature, v. 356, p. 673–678.
Knoll, A.H., Swett, K., and Mark, J., 1991, Paleobiology of a Neoproterozoic tidal flat/lagoonal complex: the Draken Conglomerate Formation, Spitsbergen: Journal of Paleontology, v. 65, p. 531–570.
Knoll, A.H., Wörndle, S., and Kah, L.C., 2013, Covariance of microfossil assemblages and microbialite textures across an upper Mesoproterozoic carbonate platform: Palaios, v. 28, p. 453–470.
Knoll, A.H., Germs, G.J.B., Tankard, A., and Welsink, H., 2020, Tonian microfossils from subsurface shales in Botswana: Precambrian Research, v. 345, n. 105779.
Kouketsu, Y., Mizukami, T., Mori, H., Endo, S., Aoya, M., Hara, H., Nakamura, D., and Wallis, S., 2014, A new approach to develop the Raman carbonaceous material geothermometer for low-grade metamorphism using peak width: Island Arc, v. 23, p. 33–50.
Kumar, A., and Venkatachala, B.S., 1998, Proterozoic chert microbiota from the Riasi Inlier of the Vaishnodevi Limestone in the Himalayan Foot-hills, Jammu, India: Indian Journal of Petroleum Geology, v. 7, p. 51–70.
Kumar, S., and Pandey, S.K., 2008, Discovery of organic-walled microbiota from the black-bedded chert, Balwan Limestone, the Bhander Group, Lakheri area, Rajasthan: Current Science, v. 94, p. 797–800.
Kumar, S., and Srivastava, P., 1995, Microfossils from the Kheinjua Formation, Mesoproterozoic Semri Group, Newari area, central India: Precambrian Research, v. 74, p. 91–117.
Lamb, D.M., Awramik, S.M., Chapman, D.J., and Zhu, S., 2009, Evidence for eukaryotic diversification in the ~1800 million-year-old Changzhougou Formation, North China: Precambrian Research, v. 173, p. 93–104.
Lei, Y., Shen, J., Algeo, T.J., Servais, T., Feng, Q., and Yu, J., 2019, Phytoplankton (acritarch) community changes during the Permian–Triassic transition in South China: Palaeogeography, Palaeoclimatology, Palaeoecology, v. 519, p. 84–94.
Le Rosq, C.R., 2021, rampy. https://github.com/charlesll/rampy (accessed Jul 2021).
Liais, E., 1872. Climat, géologie, faune et géographie botanique du Brésil, VIII. Paris, Georges Chamerot.
Li, G., Pang, K., Chen, L., Zhou, G., Han, C., Yang, L., Wang, W., Yang, F., and Yin, L., 2019, Organic-walled microfossils from the Tonian Tongjiazhuang Formation of the Tumen Group in western Shandong, North China Craton and their biostratigraphic significance: Gondwana Research, v. 76, p. 260–289.
Liu, P., and Moczydłowska, M., 2019, Ediacaran microfossils from the Doushantuo Formation chert nodules in the Yangtze Gorges area, South China, and new biozones: Fossils and Strata, v. 65, 172 p.
Liu, P., Xiao, S., Yin, C., Chen, S., Zhou, C., and Li, M., 2014, Ediacaran acanthomorphic acritarchs and other microfossils from chert nodules of the Upper Doushantuo Formation in the Yangtze Gorges area, South China: Paleontological Society Memoir 72, 139 p.
Loron, C., and Moczydłowska, M., 2017, Tonian (Neoproterozoic) eukaryotic and prokaryotic organic-walled microfossils from the upper Visingsö Group, Sweden: Palynology, v. 42, p. 220–254.
Loron, C.C., Rainbird, R.H., Turner, E.C., Greenman, J.W., and Javaux, E.J., 2019, Organic-walled microfossils from the late Mesoproterozoic to early Neoproterozoic lower Shaler Supergroup (Arctic Canada): diversity and biostratigraphic significance: Precambrian Research, v. 321, p. 349–374.
Loron, C.C., Halverson, G.P., Rainbird, R.H., Skulski, T., Turner, E.C., and Javaux, E.J., 2021, Shale-hosted biota from the Dismal Lakes Group in Arctic Canada supports an early Mesoproterozoic diversification of eukaryotes: Journal of Paleontology, v. 95, p. 1113–1137.
Lottaroli, F., Craig, J., and Thusu, B., 2014, Neoproterozoic–early Cambrian (Infracambrian) hydrocarbon prospectivity of North Africa: a synthesis: Geological Society, London, Special Publications, v. 326, p. 137–156.
Maithy, P.K., 1975, Micro-organisms from the Bushimay System (late Precambrian) of Kanshi, Zaire: Palaeoobotanist, v. 22, p. 33–149.
Maithy, P.K., and Shukla, M., 1977, Microbiota from the Suket Shales, Vindhyan (late Precambrian), Madhya Pradesh: Palaeobotanist, v. 23, p. 176–188.
Mandal, J., Maithy, P.K., Barman, G., and Verma, K.K., 1984, Microbiota from the Kushalgarh Formation, Delhi, India: Palaeobotanist, v. 32, p. 1–19.
Marchese, H.G., 1974, Estromatolitos "Gymnosolenidos" en el lado oriental de Minas Gerais, Brasil: Revista Brasileira de Geociências, v. 4, p. 172–190.
Marshall, C.P., Javaux, E.J., Knoll, A.H., and Walter, M.R., 2005, Combined micro-Fourier transform infrared (FTIR) spectroscopy and micro-Raman spectroscopy of Proterozoic acritarchs: a new approach to Palaeobiology: Precambrian Research, v. 138, p. 208–224.
Mazoni, A.F., 2021, Raman Online. https://github.com/alyssonmazoni/raman_online (accessed Jul 2021).
Mendelson, C.V., and Schopf, J.W., 1982, Proterozoic microfossils from the Sukhaya Tunguska, Shorikha, and Yudoma formations of the Siberian platform, USSR: Journal of the Palaeontological Society of India, v. 56, p. 42–83.
Merdith, A.S., Williams, S.E., Collins, A.S., Tetley, M.G., Mulder, J.A., et al., 2021, Extending full-plate tectonic models into deep time: linking the Neoproterozoic and the Phanerozoic: Earth-Science Reviews, v. 214, p. 2–44.
Miao, L., Moczydłowska, M., Zhu, S., and Zhu, M., 2019, New record of organic-walled, morphologically distinct microfossils from the late Paleoproterozoic Changcheng Group in the Yanshan Range, North China: Precambrian Research, v. 321, p. 172–198.
Miao, L., Moczydłowska, M., and Zhu, M., 2021, A diverse organic-walled microfossil assemblage from the Mesoproterozoic Xiamaling Formation, North China: Precambrian Research, v. 360, n. 106235.
Mikhailova, N.S., 1986, Novye nakhodki mikrofitofossilij iz otlozhenij verkhnego rifeya Krasnoyarskogo kraya *in* Sokolov, B.S., ed., Aktual 'nye Voprosy Sovremennoj: Kyiv, Naukova Dumka, p. 31–37.
Moczydłowska, M., 1991, Acritarch Biostratigraphy of the Lower Cambrian and the Precambrian–Cambrian Boundary in Southeastern Poland: Oslo, Universitetsforlaget, 127 p.
Moczydłowska, M., 2008a, New records of late Ediacaran microbiota from Poland: Precambrian Research, v. 167, p. 71–92.
Moczydłowska, M., 2008b, The Ediacaran microbiota and the survival of Snowball Earth conditions: Precambrian Research, v. 167, p. 71–92.
Moczydłowska, M., 2016, Algal affinities of Ediacaran and Cambrian organic-walled microfossils with internal reproductive bodies: *Tanarium* and other morphotypes: Palynology, v. 40, p. 83–121.
Moczydlowska, M., Landing, E., Zang, W., and Palacios, T., 2011, Proterozoic phytoplankton and timing of chlorophyte algae origins: Palaeontology, v. 54, p. 721–733.
Morais, L., Fairchild T.R., Freitas, B.T., Rudnitzki, I.D., Silva, E.P., Lahr, D., Moreira, A.C., Abrahão Filho, E.A., Leme, J.M., and Trindade, R.I.F., 2021, Doushantuo-Pertatataka-like acritarchs from the late Ediacaran Bocaina Formation (Corumbá Group, Brazil): Frontiers in Earth Science, v. 9, n. 787011, https://doi.org/10.3389/feart.2021.787011.
Moreira, D.S., Uhlein, A., Dussin, I.A., Uhlein, G.J., and Misuzaki, A.M.P., 2020, A Cambrian age for the upper Bambuí Group, Brazil, supported by the first U–Pb dating of volcaniclastic bed: Journal of South American Earth Sciences, v. 99, n. 102503.
Nagovitsin, K.E., and Kochnev, B.B., 2015, Microfossils and biofacies of the Vendian fossil biota in the southern Siberian Platform: Russian Geology and Geophysics, v. 56, p. 584–593.
Naumova, S.N., 1949, Spores of the lower Cambrian: Izvestiya Akademii Nauk SSSR, v. 4, p. 49–56.
Nemerov, V.K., Stanevich, A.M., Razvozzhaeva, E.A., Budyak, A.E., and Kornilova, T.A., 2010, Biogenic sedimentation factors of mineralization in the Neoproterozoic strata of the Baikal–Patom region: Russian Geology and Geophysics, v. 51, p. 572–586.
Nyberg, A.V., and Schopf, J.W, 1984, Microfossils in stromatolitic cherts from the upper Proterozoic Min'yar Formation, southern Ural Mountains: Journal of Paleontology, v. 58, p. 738–772.
Oehler, J.H., 1977, Microflora of the H.Y.C. Pyritic Shale Member of the Barney Creek Formation (McArthur Group), middle Proterozoic of Northern Australia: Alcheringa, v. 1, p. 315–349.

Okubo, J., Warren, L. V., Luvizotto, G.L., Varejão, F.G., Quaglio, F., Uhlein, G.J., and Assine, M.L., 2020, Evidences of seismic events during the sedimentation of Sete Lagoas Formation (Bambuí Group—Ediacaran, Brazil): Journal of South American Earth Sciences, v. 98, n. 102461.

Oliveira, A.I., and Leonardos, O.H., 1943, Geologia Do Brasil: Rio de Janeiro, Serviço de Informação Agrícola, 813 p.

Ouyang, Q., Guan, C., Zhou, C., and Xiao, S., 2017, Acanthomorphic acritarchs of the Doushantuo Formation from an upper slope section in northwestern Hunan Province, South China, with implications for early–middle Ediacaran biostratigraphy: Precambrian Research, v. 298, p. 512–529.

Ouyang, Q., Zhou, C., Xiao, S., Guan, C., Chen, Z., Yuan, X., and Sun, Y., 2021, Distribution of Ediacaran acanthomorphic acritarchs in the lower Doushantuo Formation of the Yangtze Gorges area, South China: evolutionary and stratigraphic implications: Precambrian Research, v. 353, n. 106005.

Ouyang, S., Yin, L., and Zaiping, L., 1974, Sinian and Cambrian spores and acritarchs, in Press, S., ed., Handbook of the Stratigraphy and Paleontology of South Western China: Beijing, Science Publishing House, p. 72–80, 114–123.

Palacios, T., 1989, Microfósiles de Pared Orgánica Del Proterozoico Superior (Región Central de La Península Ibérica): Memorias del Museo Paleontológico de la Universidad de Zaragoza, 91 p.

Pandey, S.K., and Kumar, S., 2013, Organic walled microbiota from the silicified algal clasts, Bhander limestone, Satna area, Madhya Pradesh: Journal of the Geological Society of India, v. 82, p. 499–508.

Pang, K., Tang, Q., Wu, C., Li, G., Chen, L., Wan, B., Yuan, X., Bodnar, R.J., and Xiao, S., 2020, Raman spectroscopy and structural heterogeneity of carbonaceous material in Proterozoic organic-walled microfossils in the North China Craton: Precambrian Research, v. 346, n. 105818.

Paula-Santos, G.M., Babinski, M., Kuchenbecker, M., Caetano-Filho, S., Trindade, R.I.F., and Pedrosa-Soares, A.C., 2015, New evidence of an Ediacaran age for the Bambuí Group in southern São Francisco craton (eastern Brazil) from zircon U–Pb data and isotope chemostratigraphy: Gondwana Research, v. 28, p. 702–720.

Perrella Júnior, P., Uhlein, A., Uhlein, G.J., Sial, A.N., Pedrosa-Soares, A.C., and Lima, O.N.B., 2017, Facies analysis, sequence stratigraphy and chemostratigraphy of the Sete Lagoas Formation (Bambuí Group), northern Minas Gerais State, Brazil: evidence of a cap carbonate deposited on the Januária basement high: Brazilian Journal of Geology, v. 47, p. 59–77.

Peterson, K.J., and Butterfield, N.J., 2005, Origin of the Eumetazoa: testing ecological predictions of molecular clocks against the Proterozoic fossil record: Proceedings of the National Academy of Sciences of the United States of America, v. 102, p. 9547–9552.

Pimentel, M.M., and Fuck, R.A., 1992, Neoproterozoic crustal accretion in central: Geology, v. 20, p. 375–379.

Pimentel, M.M., Rodrigues, J.B., DellaGiustina, M.E.S., Junges, S., Matteini, M., and Armstrong, R., 2011, The tectonic evolution of the Neoproterozoic Brasília Belt, central Brazil, based on SHRIMP and LA-ICPMS U-Pb sedimentary provenance data: a review: Journal of South American Earth Sciences, v. 31, p. 345–357.

Porter, S.M., and Riedman, L.A., 2016, Systematics of organic-walled microfossils from the ca. 780–740 Ma Chuar Group, Grand Canyon, Arizona: Journal of Paleontology, v. 90, p. 815–853.

Prasad, B., Uniyal, S.N., and Asher, R., 2005, Organic-walled microfossils from the Proterozoic Vindhyan Supergroup of Son Valley, Madhya Pradesh, India: Palaeobotanist, v. 54, p. 13–60.

Prasad, B., Asher, R., and Borgohai, B., 2010, Late Neoproterozoic (Ediacaran)–early Paleozoic (Cambrian) Acritarchs from the Marwar Supergroup, Bikaner-Nagaur Basin, Rajasthan: Journal of the Geological Society of India, v. 75, p. 415–431.

Pykhova, N.G., 1973, Dokembriskie akritarhi Moskovskogo graben I Yuzhnogo: Obshchestva Ispitateli Prirody Otdel Geologicheskii Novaya, v. 48, p. 91–107.

Qu, Y., Engdahl, A., Zhu, S., Vajda, V., and McLoughlin, N., 2015, Ultrastructural heterogeneity of carbonaceous material in ancient cherts: investigating biosignature origin and preservation: Astrobiology, v. 15, p. 825–842.

Reis, H.L.S., and Alkmim, F.F., 2015, Anatomy of a basin-controlled foreland fold-thrust belt curve: the Três Marias salient, São Francisco basin, Brazil: Marine and Petroleum Geology, v. 66, p. 711–731.

Reis, H.L.S., and Suss, J.F., 2016, Mixed carbonate–siliciclastic sedimentation in forebulge grabens: an example from the Ediacaran Bambuí Group, São Francisco Basin, Brazil: Sedimentary Geology, v. 339, p. 83–103.

Riedman, L.A., Porter, S.M., and Calver, C.R., 2018, Vase-shaped microfossil biostratigraphy with new data from Tasmania, Svalbard, Greenland, Sweden and the Yukon: Precambrian Research, v. 319, p. 19–36.

Rimann, E., 1917, A Kimberlita no Brazil: Anais Da Escola de Minas Gerais, v. 15, p. 27–32.

Rodrigues, J.B., 2008, Proveniência de sedimentos dos grupos Canastra, Ibiá, Vazante e Bambuí - Um estudo de zircões detríticos e idades modelos Sm-Nd [Ph.D. thesis]: Brasília, Brazil, Universidade de Brasília, 128 p.

Samuelsson, J., and Butterfield, N.J., 2001, Neoproterozoic fossils from the Franklin Mountains, northwestern Canada: stratigraphic and palaeobiological implications: Precambrian Research, v. 107, p. 235–251.

Sanchez, E.A.M., and Fairchild, T.R., 2018, Reavaliação De Fósseis Do Grupo Bambuí: Implicações Paleobiológicas Para O Neoproterozoico Tardio Do Brasil: Geonomos, v. 25, https://doi.org/10.18285/geonomos.v25i2.1076.

Sanchez, E.A.M., Uhlein, A., and Fairchild, T.R., 2021, *Treptichnus pedum* in the Três Marias Formation, south-central Brazil, and its implications for the Ediacaran–Cambrian transition in South America: Journal of South American Earth Sciences, v. 105, n. 102983.

Schopf, J.W., 1968, Microflora of the Bitter Springs Formation, late Precambrian, central Australia: Journal of Paleontology, v. 42, p. 651–688.

Schopf, J.W., Sergeev, V.N., and Kudryavtsev, A.B., 2015, A new approach to ancient microorganisms: taxonomy, paleoecology, and biostratigraphy of the lower Cambrian Berkuta and Chulaktau microbiotas of South Kazakhstan: Journal of Paleontology, v. 89, p. 695–729.

Seilacher, A., 1955, Spuren und fazies im Unterkambrium, *in* Schindewolf, O.H., and Seilacher, A., eds., Beitrage zur Kenntnis des Kambriums in der Salt Range (Pakistan), Abhandlungen 10, Mainz: Akademie der Wissenschaften und der Literatur zu Mainz, Mathematisch Naturwissenschaftliche Klasse, p. 373–399.

Sergeev, V.N., 1984, Microfossils in the silicified columnar stromatolites from the upper Riphean deposits of the Turukhansk Uplift: Doklady AN SSSR, v. 278, p. 436–440.

Sergeev, V.N., 1992, Silicified Microfossils from the Precambrian and Cambrian Deposits of the Southern Ural Mountains and Middle Asia: Moscow, Nauka, 134 p.

Sergeev, V.N., 1994, Microfossils in cherts from the middle Riphean (Mesoproterozoic) Avzyan Formation, southern Ural Mountains, Russian Federation: Precambrian Research, v. 65, p. 231–254.

Sergeev, V.N., 2001, Paleobiology of the Neoproterozoic (upper Riphean) Shorikha and Burovaya Silicified Microbiotas, Turukhansk Uplift, Siberia: Journal of Paleontology, v. 75, p. 427–448.

Sergeev, V.N., 2006, Precambrian Microfossils in Cherts: Their Paleobiology, Classification, and Biostratigraphic Usefulness: Moscow, Geos, 280 p.

Sergeev, V.N., and Lee, S.-J., 2001, Microfossils from cherts of the middle Riphean Svetlyi Formation, the Uchur–Maya Region of Siberia and their stratigraphic significance: Stratigraphy and Geological Correlation, v. 9, p. 1–10.

Sergeev, V.N., and Lee, S.-J., 2004, New data on silicified microfossils from the Satka Formation of the lower Riphean Stratotype, the Urals: Stratigraphy and Geological Correlation, v. 12, p. 1–21.

Sergeev, V.N., and Schopf, J.W., 2010, Taxonomy, paleoecology and biostratigraphy of the late Neoproterozoic Chichkan Microbiota of South Kazakhstan: the marine biosphere on the eve of metazoan radiation: Journal of Paleontology, v. 84, p. 363–401.

Sergeev, V.N., and Seong-Joo, L., 2006, Real eukaryotes and precipitates first found in the middle Riphean stratotype, Southern Urals: Stratigraphy and Geological Correlation, v. 14, p. 1–18.

Sergeev, V.N., Knoll, A.H., Kolosova, S.P., and Kolosov., P.N., 1994, Microfossils in cherts from the Mesoproterozoic Debengda Formation, Olenek Uplift, Northeastern Siberia: Stratigraphy and Geological Correlation, v. 2, p. 23–38.

Sergeev, V.N., Knoll, A.H., and Petrov, P.Y., 1997, Paleobiology of the Mesoproterozoic–Neoproterozoic transition: the Sukhaya Tunguska Formation, Turukhansk Uplift, Siberia: Precambrian Research, v. 85, p. 201–239.

Sergeev, V.N., Sharma, M., and Shukla, Y., 2008, Mesoproterozoic silicified microbiotas of Russia and India—characteristics and contrasts: Palaeobotanist, v. 57, p. 323–358.

Sergeev, V.N., Sharma, M., and Shukla, Y., 2012, Proterozoic fossil cyanobacteria: Paleobotanist, v. 61, p. 189–358.

Sergeev, V.N., Knoll, A.H., Vorob'eva, N.G., and Sergeeva, N.D., 2016, Microfossils from the lower Mesoproterozoic Kaltasy Formation, East European Platform: Precambrian Research, v. 278, p. 87–107.

Sergeev, V.N., Vorob'eva, N.G., and Petrov, P.Y., 2017a, The biostratigraphic conundrum of Siberia: do true Tonian–Cryogenian microfossils occur in Mesoproterozoic rocks?: Precambrian Research, v. 299, p. 282–302.

Sergeev, V.N., Vorob'eva, N.G., Petrov, P.Y., and Semikhatov, M.A., 2017b, Taxonomic composition and biostratigraphic value of the early Riphean organic-walled microfossil association from the Ust'-Il'ya Formation of the Anabar Uplift, Northern Siberia: Stratigraphy and Geological Correlation, v. 25, p. 241–255.

Shang, X., Liu, P., and Moczydłowska, M., 2019, Acritarchs from the Doushantuo Formation at Liujing section in Songlin area of Guizhou Province, South China: implications for early–middle Ediacaran biostratigraphy: Precambrian Research, v. 334, n. 105453.

https://doi.org/10.1017/jpa.2023.83 Published online by Cambridge University Press

Sharma, M., and Sergeev, V.N., 2004, Genesis of carbonate precipitate patterns and associated microfossils in Mesoproterozoic formations of India and Russia—a comparative study: Precambrian Research, v. 134, p. 317–347.
Shepeleva, E.D., 1962, Rastitel'nye? ostatki neizvestnoj sistematicheskoj prinadlezhnosti iz otlozhenij bavlinskoj serii Volgo-Ural'skoj provintsii: Doklady Akademii Nauk SSSR, v. 142, p. 456–457.
Shi, M., Feng, Q., Khan, M.Z., and Zhu, S., 2017a, An eukaryote-bearing microbiota from the early Mesoproterozoic Gaoyuzhuang Formation, Tianjin, China and its significance: Precambrian Research, v. 303, p. 709–726.
Shi, M., Feng, Q., Khan, M.Z., Awramik, S.M., and Zhu, S., 2017b, Silicified microbiota from the Paleoproterozoic Dahongyu Formation, Tianjin, China: Journal of Paleontology, v. 91, p. 369–392.
Shukla, Y., Sharma, M., and Sergeev, V.N., 2020, Organic walled microfossils from the Neoproterozoic Owk Shale, Kurnool Group, South India: Palaeoworld, v. 29, p. 490–511.
Simonetti, C., and Fairchild, T.R., 1989, Paleobiologia de uma nova microflórula silicificada do Grupo Bambuí (Proterozoico Superior), da região de Unaí, MG: Boletim IG, v. 7, https://doi.org/10.11606/issn.2317-8078.v0i7p01-25.
Simonetti, C., and Fairchild, T.R., 2000, Proterozoic microfossils from subsurface siliciclastic rocks of the São Francisco Craton, south-central Brazil: Precambrian Research, v. 103, p. 1–29.
Singh, V.K., and Sharma, M., 2016, Mesoproterozoic organic-walled microfossils from the Chaporadih Formation, Chandarpur Group, Chhattisgarh Supergroup, Odisha, India: Journal of the Palaeontological Society of India, v. 61, p. 75–84.
Sommer, F.W., 1971, Microfósseis do Calcário Bambuí, de Pedro Leopoldo, Estado de Minas Gerais: Anais Da Academia Brasileira de Ciências, v. 61, p. 75–84.
Stanevich, A.M., Maksimova, E.N., Kornilova, T.A., Gladkochub, D.P., Mazukabzov, A.M., and Donskaya, T. V., 2009, Microfossils from the Arymas and Debengda formations, the Riphean of the Olenek Uplift: age and presumable nature: Stratigraphy and Geological Correlation, v. 17, p. 20–35.
Stanier, R.Y., Sistrom, W.R., Hansen, T.A., Whitton, B.A., Castenholz, R.W., et al., 1978, Proposal to place nomenclature of the Cyanobacteria (blue-green algae) under the rules of the International Code of Nomenclature of bacteria: International Journal of Systematic Bacteriology, v. 28, p. 335–336.
Strother, P.K., Battison, L., Brasier, M.D., and Wellman, C.H., 2011, Earth's earliest non-marine eukaryotes: Nature, v. 473, p. 505–509.
Suslova, E.A., Parfenova, T.M., Saraev, S. V., and Nagovitsyn, K.E., 2017, Organic geochemistry of rocks of the Mesoproterozoic Malgin Formation and their depositional environments (southeastern Siberian Platform): Russian Geology and Geophysics, v. 58, p. 516–528.
Tang, Q., Pang, K., Xiao, S., Yuan, X., Ou, Z., and Wan, B., 2013, Organic-walled microfossils from the early Neoproterozoic Liulaobei Formation in the Huainan region of North China and their biostratigraphic significance: Precambrian Research, v. 236, p. 157–181.
Tang, Q., Pang, K., Yuan, X., Wan, B., and Xiao, S., 2015, Organic-walled microfossils from the Tonian Gouhou Formation, Huaibei region, North China Craton, and their biostratigraphic implications: Precambrian Research, v. 266, p. 296–318.
Tang, Q., Hughes, N.C., McKenzie, N.R., Myrow, P.M., and Xiao, S., 2017, Late Mesoproterozoic–early Neoproterozoic organic-walled microfossils from the Madhubani Group of the Ganga Valley, northern India: Palaeontology, v. 60, p. 869–891.
Tang, Q., Hu, J., Xie, G., Yuan, X., Wan, B., et al., 2019, A problematic animal fossil from the early Cambrian Hetang Formation, South China—a reply: Journal of Paleontology, v. 93, p. 1279–1282.
Tang, Q., Pang, K., Li, G., Chen, L., Yuan, X., Sharma, M., and Xiao, S., 2021, The Proterozoic macrofossil Tawuia as a coenocytic eukaryote and a possible macroalga: Palaeogeography, Palaeoclimatology, Palaeoecology, v. 576, n. 110485.
Thuret, G., 1875, Essai de classification des nostocines: Annales Des Sciences Naturelles; Botanique, v. 6, p. 372–382.
Timofeev, B. V., 1966, Micropaleophytological Investigation into Ancient Formations: Moscow and Leningrad, Nauka, 238 p.
Timofeev, B.V., Hermann, T.N., and Mikhailova, N.S., 1976, Microphytofossils of the Precambrian, Cambrian and Ordovician: Leningrad, Nauka, 106 p.
Tiwari, M., and Pant, C.C., 2004, Organic-walled microfossils from the Neoproterozoic black phosphatic stringers in the Gangolihat Dolomite, Lesser Himalaya, India: Current Science, v. 87, p. 1733–1738.
Tiwari, M., and Pant, I., 2009, Microfossils from the Neoproterozoic Gangolihat Formation, Kumaun Lesser Himalaya: their stratigraphic and evolutionary significance: Journal of Asian Earth Sciences, v. 35, p. 137–149.
Tobias, T.C., 2014, Micropaleontologia da Formação Tamengo, Eco Parque Cacimba da Saúde, Ediacarano, Grupo Corumbá, Estado de Mato Grosso do Sul, Brasil [M.Sc. thesis]: Brasília, Brazil, University of Brasília, 78 p.
Turland, N.J., Wiersema, J.H., Barrie, F.R., Greuter, W., Hawksworth, D.L., et al., 2018, International Code of Nomenclature for Algae, Fungi, and Plants (Shenzhen Code) Adopted by the Nineteenth International Botanical Congress Shenzhen, China, July 2017. Regnum Vegetabile 159: Glashütten, Koeltz Botanical Books.
Turnau, E., and Racki, G., 1999, Givetian palynostratigraphy and palynofacies: new data from the Bodzentyn Syncline (Holy Cross Mountains, central Poland): Review of Paleobotany and Palynology, v. 106, p. 237–271.
Uhlein, G.J., Uhlein, A., Pereira, E., Caxito, F.A., Okubo, J., Warren, L.V., and Sial, A.N., 2019, Ediacaran paleoenvironmental changes recorded in the mixed carbonate–siliciclastic Bambuí Basin, Brazil: Palaeogeography, Palaeoclimatology, Palaeoecology, v. 517, p. 39–51.
Vidal, G., and Moczydłowska-Vidal, M., 1997, Biodiversity, speciation, and extinction trends of Proterozoic and Cambrian phytoplankton: Paleobiology, v. 23, p. 230–246.
Virtanen, P., Gommers, R., Oliphant, T.E., Haberland, M., Reddy, T., et al., 2020, SciPy 1.0: fundamental algorithms for scientific computing in Python: Nature Methods, v. 17, p. 261–272.
Vorob'eva, N.G., and Petrov, P.Y., 2014, The genus *Vendomyces* Burzin and facies—ecological specificity of the Staraya Rechka Microbiota of the late Vendian of the Anabar Uplift of Siberia and its stratigraphic analogues: Paleontological Journal, v. 48, p. 655–666.
Vorob'eva, N.G., Sergeev, V.N., and Knoll, A.H., 2009, Neoproterozoic microfossils from the northeastern margin of the East European Platform: Journal of Paleontology, v. 83, p. 161–196.
Vorob'eva, N.G., Sergeev, V.N., and Petrov, P.Y., 2015, Kotuikan Formation assemblage: a diverse organic-walled microbiota in the Mesoproterozoic Anabar succession, northern Siberia: Precambrian Research, v. 256, p. 201–222.
Walcott, C.D., 1899, Pre-Cambrian fossiliferous formations: Geological Society of America, v. 10, p. 199–244.
Walde, D.H.G., Do Carmo, D.A., Guimarães, E.M., Vieira, L.C., Erdtmann, B., Sanchez, E.A.M., Adôrno, R.R., and Tobias, T.C., 2015, New aspects of Neoproterozoic–Cambrian transition in the Corumbá region (state of Mato Grosso do Sul, Brazil): Annales de Paléontologie, v. 101, p. 213–224.
Wan, B., Tang, Q., Pang, K., Wang, X., Bao, Z., Meng, F., Zhou, C., Yuan, X., Hua, H., and Xiao, S., 2019, Repositioning the Great Unconformity at the southeastern margin of the North China Craton: Precambrian Research, v. 324, p. 1–17.
Warren, L. V., Quaglio, F., Riccomini, C., Simões, M.G., Poiré, D.G., Strikis, N.M., Anelli, L.E., and Strikis, P.C., 2014, The puzzle assembled: Ediacaran guide fossil *Cloudina* reveals an old proto-Gondwana seaway: Geology, v. 42, p. 391–394.
Woese, C., and Fox, G., 1977, No phylogenetic structure of the prokaryotic domain: Proceedings, National Academy of Sciences of the United States of America, v. 74, p. 5088–5090.
Xiao, S., and Narbonne, G.M., 2020, The Ediacaran Period, *in* Gradstein, F.M., Ogg, J.G., Schmitz, M.D., and Ogg, G.M., eds., Geologic Time Scale 2020 (first edition): Oxford, Elsevier, p. 521–561.
Xiao, S., and Tang, Q., 2021, Part B, Volume 2, Chapter 7: Microfossils of prokaryotes (Bacteria and Archaea): research history, taphonomy, and paleobiology: Treatise Online, v. 160, p. 1–37.
Xiao, S., Jiang, G., Ye, Q., Ouyang, Q., Banerjee, D. M., Singh, B. P., Muscente, A. D., Zhou, C., and Hughes, N. C., 2023, Systematic paleontology, acritarch biostratigraphy, and $\delta^{13}C$ chemostratigraphy of the early Ediacaran Krol A Formation, Lesser Himalaya, northern India: Journal of Paleontology, v. 97, https://doi.org/10.1017/jpa.2022.7.
Xing, Y.S., and Liu, K.Z., 1973, On Sinian micro-flora in Yenliao Region of China and its geological significance: Acta Geologica Sinica, v. 1, p. 1–64.
Yan, Y., and Liu, Z., 1993, Significance of eucaryotic organisms in the microfossil flora of Changcheng System: Acta Micropalaeontologica Sinica, v. 10, p. 167–180.
Yin, L., and Guan, B., 1999, Organic-walled microfossils of Neoproterozoic Dongjia Formation, Lushan County, Henan Province, North China: Precambrian Research, v. 94, p. 121–137.
Yin, L., and Yuan, X., 2007, Radiation of Meso-Neoproterozoic and early Cambrian protists inferred from the microfossil record of China: Palaeogeography, Palaeoclimatology, Palaeoecology, v. 254, p. 350–361.
Yin, L., Yang, R., Peng, J., and Kong, F., 2009, New data regarding acritarch biostratigraphy from the early–middle Cambrian Kaili Formation in Chuandong, Guizhou Province, China: Progress in Natural Science, v. 19, p. 107–114.
Yin, L.M., Singh, B.P., Bhargava, O.N., Zhao, Y.L., Negi, R.S., Meng, F.W., and Sharma, C.A., 2018, Palynomorphs from the Cambrian Series 3, Parahio valley (Spiti), Northwest Himalaya: Palaeoworld, v. 27, p. 30–41.
Zaine, M.F., 1991, Análise dos fósseis de parte da Faixa Paraguai (MS, MT) e seu contexto temporal e paleoambiental [Ph.D. thesis]: São Paulo, Brazil, Universidade de São Paulo, 215 p.
Zang, W., 1995, Early Neoproterozoic sequence stratigraphy and acritarch biostratigraphy, eastern Officer Basin, South Australia: Precambrian Research, v. 74, p. 119–175.

Zang, W., and Walter, M.R., 1992, Late Proterozoic and early Cambrian microfossils and biostratigraphy, northern Anhui and Jiangsu, central-eastern China: Precambrian Research, v. 57, p. 243–323.
Zhang, Y., Yin, L., Xiao, S., and Knoll, A.H., 1998, Permineralized fossils from the terminal Proterozoic Doushantuo Formation, South China: Paleontological Society Memoir 72, 52 p.
Zheng, S., Clausen, S., Feng, Q., and Servais, T., 2020, Review of organic-walled microfossils research from the Cambrian of China: implications for global phytoplankton diversity: Review of Palaeobotany and Palynology, v. 276, n. 104191.
Zhou, C., Xie, G., McFadden, K., Xiao, S., and Yuan, X., 2007, The diversification and extinction of Doushantuo–Pertatataka acritarchs in South China: causes and biostratigraphic significance: Geological Journal, v. 42, p. 229–262.

Accepted: 20 September 2023

https://doi.org/10.1017/jpa.2023.83 Published online by Cambridge University Press